General Disclaimer

One or more of the Following Statements may affect this Document

- This document has been reproduced from the best copy furnished by the organizational source. It is being released in the interest of making available as much information as possible.

- This document may contain data, which exceeds the sheet parameters. It was furnished in this condition by the organizational source and is the best copy available.

- This document may contain tone-on-tone or color graphs, charts and/or pictures, which have been reproduced in black and white.

- This document is paginated as submitted by the original source.

- Portions of this document are not fully legible due to the historical nature of some of the material. However, it is the best reproduction available from the original submission.

FINAL REPORT

for

A LOW-ALTITUDE SATELLITE INTERACTION STUDY

(NEUTRAL GASES)

Contract No. NAS5-11241

Prepared by

RCA
Astro-Electronics Division
Princeton, New Jersey

for

National Aeronautics and Space Administration
Goddard Space Flight Center
Greenbelt, Maryland 20771

FINAL REPORT

for

A LOW-ALTITUDE SATELLITE INTERACTION STUDY

(NEUTRAL GASES)

Contract No. NAS5-11241

Goddard Space Flight Center

Contracting Officer: George Caponiti
Technical Monitor: A. E. Hedin 621

Prepared by

RCA
Astro-Electronics Division
Princeton, New Jersey

Authors: R. R. McKinley
G. K. Bienkowski
S. M. Siskind

Project Manager: J. M. L. Holman

for

National Aeronautics and Space Administration
Goddard Space Flight Center
Greenbelt, Maryland 20771

AED R-3635-F

Issued: October 20, 1970

PREFACE

This is the final report on the Low-Altitude Satellite Interaction Study (Neutral Gases). The study was conducted by the Astro-Electronics Division of RCA for the National Aeronautics and Space Administration under Contract No. NAS5-11241. Work on the study was accomplished during the period from August 26, 1969 through September 15, 1970.

SUMMARY

Many processes and reactions relevant to the understanding of the earth's atmosphere take place in the altitude range from 90 to 150 kilometers. To obtain data in this regime, it is necessary to use rapidly moving vehicles such as rockets and low perigee satellites. However, for typical vehicle dimensions, the resultant data cannot be related to flow-field conditions using either free-molecular or high-Reynold -number continuum theory. Except for the recently developed Monte Carlo direct simulation technique, other theoretical methods are sufficiently limited that their extension to realistic cases is beyond the current "state-of-the-art".

This report documents the work done for NASA on a Monte Carlo numerical computer technique for describing the interaction of the flow-field with a spacecraft in the so-called "transitional flow regime". The current study had four major objectives, all of which were successfully completed. These were:

- To convert an existing two-dimensional, two-fluid computer program to a more general three-dimensional program capable of accommodating realistic satellite geometries,
- To couple this program to a previously existing program for determining conditions in a cavity within a satellite moving in the transitional region,
- To test the new programs using realistic data and a realistic satellite geometry, and
- To examine the possibilities of constructing a computer program capable of handling three different species of gas rather than two.

These objectives are more fully discussed in Section II of this report.

The resultant, state-of-the-art computer programs are discussed in Section III, and Section IV, paragraphs A and B. The remainder of Section IV gives the results obtained from investigating the Atmosphere Explorer spacecraft geometry over the range of conditions expected in the 90 to 150 kilometer region of the atmosphere.

The following conclusions are based on computer runs:

- The three-dimensional programs are capable of generating the data necessary for basic satellite and instrument design.

- There is a great increase of flux, over the free-stream values, at the leading edge of the satellite.
- The ratio of the heavy-to-light species increases dramatically over its free-stream value at the leading edge of the body.
- The percentage of particles reaching the body's surface directly from the free-stream decreases appreciably with decreasing altitude.

These conclusions, along with several others, are amplified in Section V of this report.

Recommendations for future work, based upon the results of this study, are made in Section VI. Briefly, these are to:

(1) Improve the current computer program model to allow for the effects of:

- Dissociation and chemical reactions induced by the vehicle's motion,
- Velocity-dependent collisional cross-sections, and
- Internal structures in molecules.

(2) Use the existing computer programs to obtain design and instrumentation data for satellites such as Atmosphere Explorer. The following information is obtainable from the current programs:

- Measurement errors as a function of altitude,
- Instrument measurements errors as a function of position on the satellite, and
- Instrument accuracies as a function of orifice and cavity size and shape.

TABLE OF CONTENTS

LIST OF ILLUSTRATIONS

LIST OF ILLUSTRATIONS (Continued)

LIST OF TABLES

SECTION I

INTRODUCTION

Many important processes which determine the properties of the earth's atmosphere occur in the lower region of the thermosphere (at altitudes between 90 and 150 kilometers above the earth's surface). Atmospheric composition in this region changes rapidly with altitude and a number of physical and chemical phenomena play a role in determining this composition. For instance, the concentration of atomic oxygen at these altitudes is determined by the absorption of solar radiation as well as the recombination and diffusion rates. Data from this region are critical to an understanding of the transition from the upper layer of the homosphere to the lower levels of the thermosphere. The National Aeronautics and Space Administration (NASA), therefore, currently is devoting considerable effort to increasing knowledge of the properties of these altitudes.

Only sounding rockets and low perigee satellites provide direct access to the 90 to 200 kilometer region of the atmosphere. Except near apogee of the sounding rocket, both of these vehicles generally move at high speed compared to the thermal speed in the atmosphere. For a typical satellite in this altitude regime, the ratio of satellite velocity to thermal speed is generally around 20. At these speeds, any significant number of collisions between incoming particles and those reflected from the body can produce extreme changes in the environment near the surface of the measuring instrument compared with that existing in the ambient atmosphere.

For a vehicle of typical dimensions (that is one to two meters in diameter), the following conditions hold. At altitudes above 150 kilometers (nominal) the mean free path of the particles is much larger than vehicle size. The particle-particle collision process in the vicinity of the vehicle need not be considered and the relation of measurements to atmospheric properties is explained in a relatively straightforward manner through free-molecular theory. Below 90 kilometers, the mean free path is so much smaller than vehicle dimensions that the fluid can be treated as a continuum with limited influence of transport properties, such as viscosity and heat conductivity. Data interpretation, although more difficult, can be performed within the realm of the extensive volume of information available on continuum, high-Reynolds-number fluid mechanics and the properties of the atmosphere can again be inferred.

However, between these two zones is a regime in which neither of the limiting theories is applicable. Any theoretical formulation in this regime must be based on kinetic theory (i.e., the flow-field must be treated from the molecular viewpoint), while useful results can only be related to the molecular behavior on a statistical basis. Most of the theoretical techniques in the transitional flow regime are of sufficiently limited nature that their extension to a multi-constituent gas and practical geometries is beyond the present state-of-the-art. A direct simulation Monte-Carlo computer technique originally developed by G. A. Bird[1] is, however, sufficiently simple in principle and efficient in operation to allow its extension to the situation described above, using present generation computers.

In March of 1967, RCA initiated a NASA funded study of the vehicle-environment interaction in the transitional flow regime, with primary emphasis on information necessary for instrument design and data interpretation.

Under this contract, NAS 5-11016 (documented in the final contract report, NASA-CR-94922[2]), a basic numerical program was developed for solving for various physical parameters necessary to describe the flow field. Two techniques were initially tested: (1) a perturbation approach and (2) a Monte Carlo approach based on Bird's direct simulation technique. When the perturbation approach proved to be valid in only the upper portion of the transitional flow region, it was abandoned in favor of the more general Monte Carlo method. The resultant initial computer program, adapted from the computer technique developed by Bird[1, 3], applied to only very simplified, two-dimensional, two-fluid situations. A sphere and an infinite cylinder were examined in some detail (each geometry requiring a separate computer program). The significant physical results obtained from this study were the following:

> A large increase in the flux and number ratios of the heavy-to-light species of particles at the leading edge of the test body compared with their free-stream ratios,
>
> A marked increase in the total particle flux at the leading edge of the test body, and
>
> A proof of the necessity of programs such as this in analyzing aerodynamic data from the 90 to 150 kilometer region of the atmosphere.

Under a second study contract, NAS 5-11145, the computer program was reorganized and divided into subroutines, making it possible to treat in a single computer program any axi-symmetric body defined by a series of quadratic equations. The main limitation of this program was the requirement that the

body axis of symmetry be aligned with its velocity vector. Other results of the second study, (described in the final contract report, NAS-CR-103666[4]) are the following:

A three-dimensional, internal flow program for examining particle disturbances in a cavity within a satellite was prepared,

Techniques for synthesizing a composite, three-species gas were explored. When this proved to be possible, several test cases were examined using a mixture with two major constituents of similar masses along with a trace gas of appreciably different mass, and

The feasibility of a more generalized, three-dimensional computer program was demonstrated.

This report documents the results of a third study contract, and in particular describes the extension of the previously developed program to three dimensions as required to investigate realistic spacecraft and sounding rocket geometries. The coupling of external fluxes, density changes, etc., to the conditions in a cavity inside the body, with an orifice on its surface, is also described.

SECTION II

OBJECTIVES

This third study contract is a direct result of the recommendations made in previous work. The major objectives of this contract are fourfold:

1. To prepare a three-dimensional external flow program,
2. To obtain realistic data for internal-external program coupling,
3. To test the applications of the new programs, and
4. To investigate the possibilities of constructing an operational, three-dimensional, three-fluid computer program.

Each of these objectives is discussed in some detail below.

A. THE THREE DIMENSIONAL EXTERNAL FLOW PROGRAM

The major task during this study was to convert the external flow program from a restricted two-dimensional program to a three-dimensional program capable of analyzing the flow fields around any axi-symmetric shape* for any angle of attack relative to the axis of symmetry of the body.

This change required a major modification in the existing program since completely new sample space geometries became necessary as did almost an entire set of new variables. Also, a method had to be found for either rotating the test body within the sample space or for introducing new particles, via a distribution function, along all the sample space boundaries. (See also the discussion in Section III.) Additionally, new output and input information was required, necessitating the addition of several new print subroutines and new formats for data presentation.

B. INTERNAL-EXTERNAL PROGRAM COUPLING

The second objective was to obtain realistic data for the internal flow program matched to the external flow conditions. It was decided that the best method for doing this was to have the internal flow input velocity distribution generated directly, in the form of output, from the external flow program. This internal-external coupling was a necessity when investigating realistic cavity shapes and locations within a satellite.

---

* In actuality, this is limited to those axi-symmetric shapes which can be divided into sections, each representable by a second order equation. In practical cases this analytical constraint should cause no difficulty.

In the previous study[4], it was not possible to match the input velocity distribution for the internal flow program with external conditions. This made it virtually impossible to study the small-scale effects of varying the internal flow geometry. Coupling the two programs allows the experimenter to put the orifice of his cavity at any position on the surface of a test satellite and to get the specific velocity distribution relevant to that position. Also, additional information is now readily available to the experimenter for relating the sensitivity of his experimental results to the position and size of the orifice of his test instrument.

C. APPLICATIONS OF THE NEW PROGRAMS

In order to gain insight into the physical processes taking place in the transitional flow region, a complete set of tests was to be done on a sample geometry. The tests actually performed covered a realistic range of values for the various parameters required to understand the flow field. Among the parameters varied were: Knudsen number*, Mach number, particle mass ratio and diameter ratio, angle of attack, and gas number density ratio.

As a further application, the new three-dimensional programs were to be used to analyze a satellite mission specified by NASA, Goddard Space Flight Center (GSFC), using best values of the expected real-flight conditions the test vehicle would experience during its actual mission. Data produced by the external flow program for a range of variations of several input parameters was examined; selected results were then used as inputs for the internal flow program to examine conditions in a cavity of prescribed shape.

In order to save computer time (an average program runs about fifty minutes), and to maximize the amount of data available for the GSFC-supplied test case, it was decided that the general test runs of the program would be made using the GSFC-supplied geometry. The geometry chosen was that of the Atmosphere Explorer satellites, given in the GSFC Specification for Atmosphere Explorers AE-C and -D[5].

D. THE THREE-FLUID PROGRAM

The possibilities of constructing an operational three-dimensional, three-fluid computer program were to be investigated. It was previously shown[4] that a three-species gas could be modeled using the two-dimensional, two-fluid program. The current applications of the three-dimensional computer program were, therefore, completed using the same modeling of the three species.

---

* The Knudsen number is defined as the ratio of particle mean-free-path to body size. It therefore increases with altitude.

When the fluid is treated as a mixture of inert gasses (no dissociation or chemical reactions), such modeling can be adequate, especially if one of the fluids of interest is a minor constituent. If dissociation or chemical reactions induced by the vehicle motion are to be treated, it is clear that three fluids must be used and modeling by two-fluid analogs becomes of dubious value.

Extension of the programs to deal with three fluids is straightforward in theory but is expected to strain the storage capabilities of the 360-91 computer and will lead to a large increase in running time.

E. DOCUMENTATION

Documentation was to be prepared for the three-dimensional, two-fluid internal-flow and external-flow computer programs. A final contract report and monthly progress reports were also to be written.

SECTION III

DEVELOPMENT OF THE THREE-DIMENSIONAL PROGRAMS

The basic theoretical foundations of Monte Carlo direct simulation techniques, as used in this study, are described in References 2 and 4; only a brief recounting of the method will be presented here. The major emphasis will be on new additions to the programs. The external and internal flow programs are discussed separately.

A. THE EXTERNAL FLOW PROGRAM

In using a Monte Carlo direct simulation method to get values for physical parameters in the transitional flow region, the approach is to conduct numerical experiments with a model gas on a large computer. The real gas is simulated by a quantity of approximately ten thousand hard-sphere molecules, which may be thought of as a representative sample of the billions of molecules in the corresponding real gas. By randomly selecting properties for the test molecules from the gross properties of the gas, the simulation is completed. Initially the molecules are distributed uniformly over the sample space with velocity components randomly selected from a distribution function appropriate to a gas in Maxwellian equilibrium and moving at the required free-stream velocity.

At time zero, the satellite test geometry is inserted into the flow and the molecules are allowed to move and collide among themselves and with the test body. Post-collision velocities are, of course, again randomly selected with the provision that momentum and energy be conserved. The move and collide processes are uncoupled by computing the collisions appropriate to a time interval, Δt, and then by moving the molecules through distances appropriate to Δt at their instantaneous velocities. The errors introduced into the molecular paths by this approximation are small as long as Δt is small compared with the mean time between collisions and is less than a typical transit time per cell. After the system reaches steady-state, useful information can be accumulated about the specific test geometry and the flow field.

A fundamental difficulty in solving the problem of converting to a three-dimensional program is deciding the manner in which to implement angles of attack other than zero degrees*. Two methods initially showed promise. In one, the body would be rotated within the sample space, and the previously used boundary

---

* The angle of attack is defined, in this study, as the angle between the flow direction and the axis of symmetry. For the Atmosphere Explorer geometry, the flow will nominally be normal to the axis of symmetry which, for the computer program, corresponds to a 90 degree angle of attack.

conditions would be applied: in the other, the body axis-of-symmetry and the sample space axis would coincide, and the boundary conditions would be modified to a form which would be valid for flow direction at an arbitrary angle to the body axis. While the former method initially appears to be less complex, the latter method was selected as the more straightforward extension of the available program.

Test calculations showed that both methods would, in effect, give the same results. The selected method had the advantage of not drastically altering the manner in which the sample space was divided into cells and it did not affect the one-to-one relationship between cells near the body and segments on the body's surface.

Upon implementing this new procedure and attempting test runs at an angle of attack of 90 degrees, problems developed in attaining adequate statistical samples on all segments of the body within the expected amount of computer running time. These problems were resolved by making two changes. The most significant change was in the manner in which new molecules were introduced into the sample space. In previous programs, each new molecule was randomly placed anywhere along a given boundary. Therefore, if only a small number of molecules were added in a given time interval, statistically they could not be expected to have an even distribution. However, when considering that the real gas, as represented by the sample particles, would have tens of thousands of molecules entering the volume rather than the ten to fifteen samples molecules, one would expect the incoming molecules to have a relatively even distribution (since the gas density is uniform). To assure a more even distribution, the program has been changed such that if N particles are to be introduced along a given boundary of length X in a given small time interval, Δt, X is divided into N segments and each of the particles is randomly placed within a separate boundary segment of length X/N. This process assures small scale randomness within a relatively even overall distribution of molecules.

The second change made was to increase the total amount of computer time allotted for each run to assure enough particles in each sample segment. These two changes allow the current program to give adequate data samples at any angle of attack.

B. THE INTERNAL FLOW PROGRAM

In order to successfully couple the internal and external flow programs, several changes were necessary in each program. After looking at the properties of both free-stream and interacted molecules independently (see for example, Figure 19) it was obvious that no single distribution function could adequately describe the

properties of both types of molecules. To circumvent this problem it was decided that the most physically correct method would be to use two independent velocity distribution functions*, one for those molecules having free-stream properties and the other for molecules which have interacted with the body or with reflected molecules.

In the external-flow computer program, a velocity sample is determined for both the free-stream and the interacted molecules. Molecules are considered free-stream or interacted according to the following, physically justified scheme: initially all molecules are considered free-stream. As time begins, after any molecule hits the body it is then considered as an "interacted" molecule. Also, free-stream molecules colliding with interacted molecules then become interacted molecules.

On any user-specified number of body-surface segments, a count is made of the total number of free-stream and interacted molecules colliding with the segment of interest. The velocity of each collision is also monitored. At the end of the run (and at certain interim times) a normalized velocity sample is printed out for both the free-stream and the interacted molecules. This velocity sample is in tabular form. A user-specified velocity range is defined by a number of equally-spaced velocity values. The table lists the velocity values along with the fractional number of colliding molecules whose velocities are less than the tabulated values. The fractions of free-stream and interacted molecules are also printed out. This information is used as input for the internal flow program. A polynomial fit subroutine was added to the internal flow program. The input velocity sample is curve-fitted by this subroutine with an m-th order polynomial (m being a user-specified integer). The coefficients of this fitted curve are then used to generate the velocity distributions of the molecules at the orifice opening, and the program proceeds essentially the same as in the older versions.

In previous versions of the program, it was required that the velocity distribution function be symmetric about a plane. All calculations were then done considering only half of the cavity (the assumption being made that since the velocity distribution function was symmetric, the interactions within the cavity would also be symmetric). However, with two independent distribution functions, it could not be assumed that both were symmetric around the same plane (or even that both were symmetric). To eliminate this problem, the internal flow program was changed to allow for calculations throughout the complete 360-degree volume of the cavity.

---

* These are actually six distribution functions for each species since the three rectangular components of each of the two functions are defined separately.

No attempt was made to physically combine the two programs. If this were done, the freedom to lengthen the running time or to reject completely the results of any specific external flow program, before proceeding with a lengthy internal flow calculation, would be lost.

SECTION IV

RESULTS

A. THE EXTERNAL-FLOW COMPUTER PROGRAM

Much of the effort of the current study went into the writing and debugging of the three-dimensional, two-fluid, Monte Carlo external flow computer program. The computer program itself is one of the major results of this study. Complete documentation of this program is being forwarded to NASA under separate cover[6]. This program is based on and adapted from a previously developed program, SONIC I[7]. A description of some of the major differences between the two programs and the reason for these differences is given in the paragraphs below.

Initially, in order to facilitate debugging efforts and to make large numbers of production runs easier to prepare, several internal changes were made in the program. Most of the dimensioned variables were removed from the previously existing COMMON statements and are now defined by DIMENSION statements only in the subroutines in which they are required. Additionally, all of the input parameters to the program are in NAMELIST format rather than in the more structured format used in past programs. All of these parameters are now given preset values within the program, and it is necessary to input only those parameters which the user wishes to define as other than the preset values. These changes make it considerably easier to increase or decrease the total running time and to make the overall computer program larger or smaller.

In the external flow program, the three-dimensional sample space is now divided into about eight-hundred cells of varying sizes; the smaller cells being at the leading edge of the body. The cell sizes are selected such that the expected change in flow properties over the width of each cell is small. A typical cell geometry is shown in Figure 1. As can be seen from this figure, the major change from the two-dimensional program is that the previously assumed concentric annular cells are now segmented angularly by planes coming radially outward from the axis of symmetry of the body. It is also possible to put more angular segments at the leading edge of the body where, for large angles of attack, much more interaction takes place.

In the current program, as in the preceding versions, many of the calculations are done on a cell-by-cell basis. Many of the larger cells are subdivided into smaller cells and the test body also replaces some of the cells near the center of the sample space. These subdivided or replaced cells are then given a volume of zero, so that no calculations are done in them. In earlier versions of the

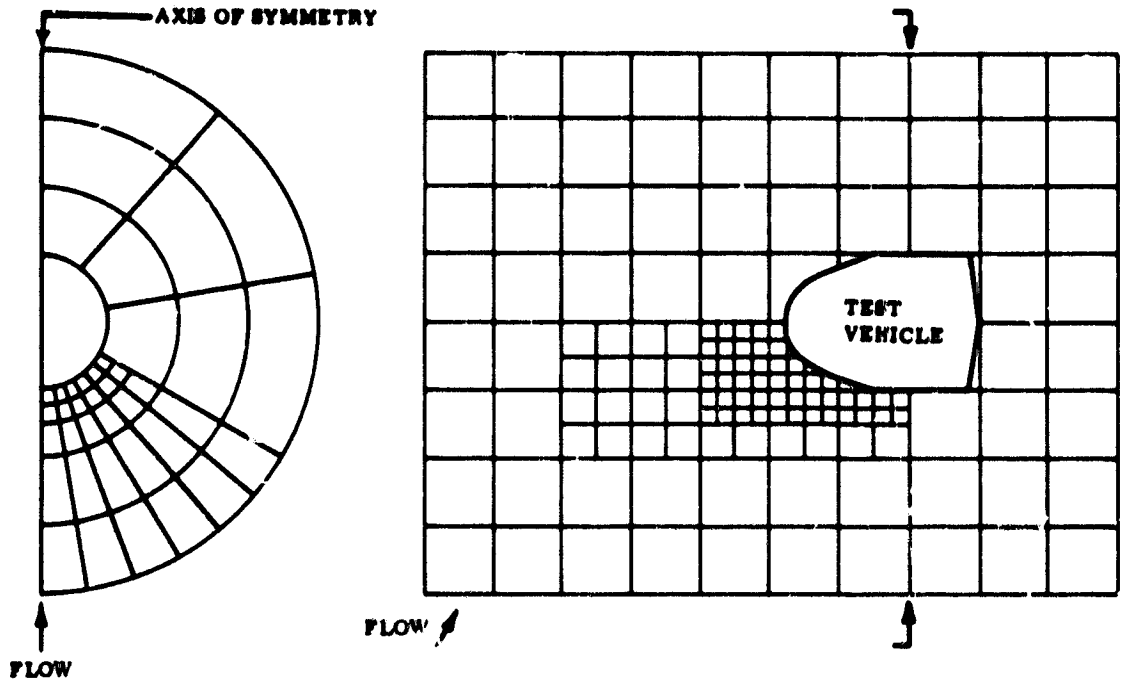

Figure 1. Typical Cell Geometry for an Axially Symmetric Body for Three Levels of Cell Size

program, it was necessary to dimension many arrays to include these zero volume cells, thereby wasting much valuable computer storage space. In the current version of the program, the cells are renumbered before starting calculations, with all cells of zero volume being omitted. Many arrays are now based on the new numbering system, thereby decreasing their size by as much as thirty percent.

In converting to a three-dimensional program, the major change with respect to individual particles was the addition of a third position coordinate. In the SONIC I program, only two position coordinates were necessary, since the system was assumed symmetric with respect to the third coordinate. The three velocity coordinates are also monitored.

Aside from the above-described general changes in the programs, significant changes were made in many of the individual subroutines. The major changes are described on a subroutine-by-subroutine basis.

1. MAIN

This segment is the major one in the program. It calls all of the subroutines and, in effect, keeps track of the program. In order to give the

program a restart capability, this segment was completely reorganized. This capability is used when the user-specified, initial number of molecules causes the maximum permitted number of molecules to be exceeded at some later time (as often happens when a new geometry or altitude is tested). Instead of causing the program to stop, thereby wasting valuable turn-around time, the initial number of molecules is now decreased by 100 and the program is restarted.

As described in Section III of this paper, velocity distribution functions for later use in the internal flow program are now determined and set up in MAIN. Additionally, Central Processing Unit time is now monitored and when thirty seconds or less remain, the calculations cease and the latest data is printed out. The number of copies of the final data set to be printed is now a user-specified number.

In order to decrease the size of MAIN, several sections of it (which are also used in other parts of the program) have been removed and are now separate subroutines. The new subroutines PRINTA and PRINTB are used to print out the initial cell volumes, positions, and centers, along with the values of many parameters used in the program. The new subroutine DIAG now contains all programmed diagnostic messages. These are intended to help the user in debugging his computer runs.

2. Subroutine FUNCTM

This new subroutine is called by the Simpson's Rule Integrator. It calculates the necessary coefficients for using a Simpson's Rule integration to obtain the flux and velocity distributions necessary for the program. These distributions were needed when it became necessary to define velocity distribution functions along all boundaries of the sample space.

3. Subroutine COLLIDE

In this subroutine an additional determination is now made for the purpose of computing the distribution functions in DRAG and for future flow-field data analysis. Each particle is considered to belong to one of three sets. All particles entering through the boundaries are initially considered to be free-stream particles. When two free-stream particles collide, both remain free-stream. A particle whose last collision was with the body is considered to be a body particle. All remaining particles not belonging to either of the two sets described above are called collided particles. For computation of surface distribution functions in DRAG, the sets of collided and body particles are considered one and are called "interacted" particles.

This change was easily included in the program by adding another variable to those used to describe each particle. If the value in this variable location is zero, the particle is a free-stream particle; if it is a one or two (two if the particles last collision was with the body, one otherwise) the particle is interacted.

4. Subroutine MOVE

In this subroutine, the particles are moved according to their latest velocity. The subroutine has been made completely three-dimensional. In the SONIC I program, MOVE considered particles in a so-called zero plane. As a particle moved out of its zero plane, it was necessary to shift the particle back to the zero plane before considering cell related calculations. Since cells are now segmented angularly, three particle coordinates are retained throughout the program.

5. Subroutine FLOW

FLOW is the subroutine which introduces new molecules into the sample volume. At other than zero angle of attack, it is necessary to add significant numbers of particles along more than one boundary. FLOW now defines velocity distribution functions along all boundaries of the sample volume. Additionally, as discussed in Section III, the new particles are added more evenly, thereby better simulating the physically expected uniform free flow conditions.

6. Subroutine DRAG

This subroutine calculates the required parameters (momentum and energy transfer) at the body in three dimensions. One section of DRAG has been removed to form the new subroutine NORMAL. NORMAL calculates the normal to the body surface at any point. It was removed from DRAG because body surface normals are now required for calculations made in other parts of the program.

The new distribution functions, needed as input for the internal flow program, are now also calculated in DRAG. When a molecule collides with one of the body-surface segments on which a velocity sample is required, its velocity and species are monitored, and the proper section of the velocity sample is increased correspondingly. A more complete description of this process is described in Section III, Paragraph B.

7. Subroutines PRINT1 Through PRINT5

These five subroutines are used for computing and printing out all of the necessary output parameters of the program.

- PRINT1 calculates and prints out the various body gross surface coefficients including heat transfer, drag, and lift.
- PRINT2 calculates and prints body parameters such as number flux, shear, pressure, and heat transfer as they are distributed over individual surface segments.
- PRINT3 prints out the velocity samples, obtained in the subroutine DRAG, for the selected body segments.
- PRINT4 computes and prints, on a cell-by-cell basis, the time-averaged, flow-field information. Among the parameters printed are: average cell velocities and temperatures, number density, and mass density.
- PRINT5 calculates and prints out the same quantities as PRINT4, but on an instantaneous basis before the steady-state time is reached.

The above list of changes for the individual subroutines is by no means complete. Also, changes made in one subroutine generally affected several other subroutines, and the general program alterations described at the beginning of this section affected virtually every subroutine. For a more comprehensive description of the new program along with a complete listing, the reader is referred to the external-flow program document.

B. THE INTERNAL-FLOW COMPUTER PROGRAM

Complete documentation of the internal flow program is being forwarded to NASA under separate cover[6]. Only the major changes in the program made during this study are described below. All of these changes were made in order to facilitate the internal-external programs coupling.

After the three-dimensional, two-fluid computer program was written, it was necessary to bring the previously existing internal flow program to a similar operational status in order to proceed with the coupling. Since the internal flow program, developed previously[4], was a three-dimensional program, the changes necessary to bring it into accord with the external flow program were not as great in scope as those necessary to convert the external flow program.

The major geometrical change, as discussed in Section III, Paragraph B, was to make the internal flow program work through 360 degrees. This being accomplished, it was necessary to introduce a polynomial-fit subroutine into the program.

The output from the external flow program, as described in preceding sections, is in the form of a velocity sample at discrete intervals, while the original internal-flow computer program required a complete velocity distribution function. This distribution function is the relative number of particles added by increasing the velocity by an amount dU for all values of U and is, in effect, the derivative of the velocity sample. However, obtaining the velocity distribution function by taking numerical derivatives of the velocity sample without first smoothing the data can lead to large statistical errors. For this reason a polynomial-fit subroutine was added to the beginning of the internal-flow program. This subroutine fits the input velocity samples with a polynomial whose order can be specified. The derivative of this polynomial can then be obtained analytically and after being normalized, yields the required distribution function used in the remainder of the internal flow program.

In order to facilitate both data reduction and design synthesis, as discussed in Section III, all of the inputs and results of the internal flow program have been normalized with respect to the free-stream results used in the corresponding external flow program. Thus, outputs of the fluxes from the external flow program (normalized to the free-stream values) are fed directly as inputs into the internal flow program. An important consideration is that the geometry of any internal flow run must be specified in terms of lengths measured in free-stream mean-free-paths. Here, care must be exercised to choose a time increment that is small compared to the expected mean-free-time within the cavity, rather than that in the free stream. (In most cases the two will be significantly different.) A reasonable estimate can be obtained by use of the simple free molecular orifice formula. This formula gives the ratio of the mean-free-time between collisions in the cavity τ_{cav} to that in the free stream τ_{fs}

$$\frac{\tau_{cav}}{\tau_{fs}} \approx \frac{1}{3.2 S_\infty \phi}$$

where S_∞ is the Mach number used in the external flow program and ϕ is the flux (normalized to the free-stream value) at the orifice. This flux is one of the input parameters of the program.

All of the outputs computed in PRINT1 and PRINT2 are normalized by the appropriate combination of external free-stream number density of the first species (N_∞), the external free-stream speed, U_∞, and mass of the first species (M_1), where appropriate. Thus, to obtain the actual dimensional value of a variable, one needs to multiply by the appropriate (dimensionally correct) combination of those free-stream quantities. For instance, surface number fluxes listed in the program need to be multiplied by the quantity $N_\infty U_\infty$ to obtain the actual number flux in particles per unit time per unit area. Surface pressures and shear results must be multiplied by $M_1 N_\infty U_\infty^2$ to obtain actual pressure and

shear in units of force per unit area. Heat flux results must be multiplied by $M_1 N_\infty U_\infty^3$. Flow-field quantities are similarly defined with number density normalized by the free-stream density N_∞, while intensive properties such as velocity and temperature are normalized by the free-stream speed of sound and temperature respectively.

Again, as is the case with the external flow program, other less significant changes are discussed in the program document.

C. APPLICATIONS OF THE NEW PROGRAMS

1. Results Obtained From The External-Flow Program

In order to reach the objectives described in Section II, Para. C, thirty-two production runs of the external flow program were completed using the Atmosphere Explorer geometry. In addition, two purely diagnostic runs (L2P and L2R), testing the sensitivity of the results to certain programmer-chosen parameters, were performed. All of the external flow runs and the corresponding labels and flow parameters are listed on Table 1. In the table, the first column gives an identifying label for each run. These labels were selected such that H-runs were run using atmospheric properties corresponding approximately to an altitude of 150 kilometers above the earth's surface, M-runs correspond approximately to an altitude of 135 kilometers, L-runs to an altitude of approximately 120 kilometers and J-runs to an altitude of approximately 110 kilometers[8]. For each run, the following parameters are listed:

Kn_L	Knudsen number, based on cylinder length,
Kn	Knudsen number, based on cylinder diameter,
S	Mach number (ratio of vehicle speed to speed of sound),
RM	Mass ratio of species 2 to species 1,
DIR	Hard-sphere-model diameter ratio of species 2 to species 1,
RN	Number density ratio in the free stream of species 2 to species 1, and
TIME	Approximate duration of the 360-91 computer run.
COMMENTS	See following text.

For most runs, which unless otherwise noted were performed for the case of the cylinder axis perpendicular to the flow (i.e., 90 degree angle of attack), the COMMENTS give the binary gas constituents being simulated. In other cases, the variation of angle of attack or other special feature is noted. The runs

TABLE I. COMPUTER RUNS PERFORMED ON ATMOSPHERE EXPLORER GEOMETRY

Label	Kn_L	Kn	S	RM	DIR	RN	Time (min)	Comments
H1	30	23	16.5	1.75	1.34	7.7	60	$0-N_2$
H2	30	23	16.5	1.75	1.34	2.0	40	$0-N_2$
HIE	30	23	16.5	1.75	1.34	2.0	50	$0-N_2$
H4	30	23	16.5	7.0	1.7	2.0	50	H_e-N_2
H5	30	23	16.5	0.875	1.0	2.0	50	0_2-N_2
H6	30	23	16.5	0.875	1.0	7.7	50	0_2-N_2
H7	30	23	16.5	0.875	1.0	2.0	50	0_2-N_2
M1	10	7.6	18.0	1.75	1.34	2.0	50	$0-N_2$
M2	10	7.6	18.0	1.75	1.34	7.7	60	$0-N_2$
M3	10	7.6	18.0	1.75	1.34	20.0	60	$0-N_2$
M4	10	7.6	18.0	7.0	1.7	20.0	50	H_e-N_2
M5	10	7.6	18.0	0.875	1.0	2.0	50	0_2-N_2
M6	10	7.6	18.0	0.875	1.0	7.7	50	0_2-N_2
M7	10	7.6	18.0	0.875	1.0	20.0	50	0_2-N_2
M8	10	7.6	30.0	1.75	1.34	7.7	60	M2 with S = 30
M9	10	7.6	10.0	1.75	1.34	7.7	60	M2 with S = 10
L1	3.0	2.3	19.6	1.75	1.34	2.0	60	$0-N_2$
L2	3.0	2.3	19.6	1.75	1.34	20.0	60	$0-N_2$
LL	3.0	2.3	19.6	1.75	1.34	7.7	60	$0-N_2$
L4	3.0	2.3	19.6	7.0	1.7	20.0	50	H_e-N_2
L5	3.0	2.3	19.6	0.875	1.0	2.0	60	0_2-N_2
L6	3.0	2.3	19.6	0.875	1.0	7.7	80	0_2-N_2
L7	3.0	2.3	19.6	0.875	1.0	20.0	60	0_2-N_2
L8	3.0	2.3	19.6	1.75	1.34	2.0	60	80° Angle/Attack
L9	3.0	2.3	19.6	1.75	1.34	2.0	60	85° Angle/Attack
J1	1.0	.76	20.0	1.75	1.34	2.0	60	$0-N_2$
J2	1.0	.76	20.0	1.75	1.34	7.7	60	$0-N_2$
J3	1.0	.76	20.0	1.75	1.34	20.0	60	$0-N_2$
J4	1.0	.76	20.0	7.0	1.7	20.0	60	$He-N_2$
J5	1.0	.76	20.0	0.875	1.0	2.0	60	0_2-N_2
J6	1.0	.76	20.0	0.875	1.0	7.7	50	0_2-N_2
J7	1.0	.76	20.0	0.875	1.0	20.0	60	0_2-N_2
L2R	3.0	2.3	19.6	1.75	1.34	20.0	60	(L2 DTM Larger)
L6R	3.0	2.3	19.6	0.875	1.0	7.7	30	(L6 Cells Smaller)

labeled HIE and LL correspond approximately to the expected N_2-O concentrations ratios at 150 and 120 kilometers respectively. All runs used diffuse surface reflection.

The runs were chosen to give information on surface and flow quantities as to their:

- Variation with Knudsen number, corresponding approximately to the 110 to 150 kilometer altitude range;
- Variation with free stream concentration of either O_2 or O from 5 percent (extrapolated to trace situations) to 33 percent;
- Variation with mass ratios of 0.875 (N_2/O_2), 1.75 (N_2/O) and 7.0 (N_2/He);
- Variation with Mach number from 1.0 to 30;
- Variation with small changes in the angle of attack near 90 degrees (80 and 85 degrees).

Because of the tremendous amount of information obtained from ever a single computer run, it has been impossible to absorb and analyze all of the data in the available time. Attention was concentrated, therefore, on those aspects of the surface fluxes and surface distribution functions that appear most important in the interpretation of flight data. Flow field quantities are presented only to the extent that they are helpful in understanding the behavior of the surface fluxes. Since one of the most important pieces of aeronomic data is the atmospheric composition, the relation between the surface number fluxes of the individual species (which can be measured with a mass spectrometer) and the corresponding "free-stream" fluxes which would be measured in free molecular flow have been stressed. (The relationship between the fluxes entering a surface orifice and the measurements obtained by an instrument located in the cavity behind the orifice is discussed in Section IV, Para. C2. Only selected data has been used in order to indicate the effects that appear to be most pronounced. The major results from the external-flow program are given graphically in Figures 2 through 23.

Figures 2a and 2b show density contours (normalized to the free stream value) for the Atmosphere Explorer geometry (short cylinder transverse to the flow) in the mid-plane. The results shown are for a typical mixture density and are not too sensitive to concentration ratio or mass ratio of the constituents. Except very near the cylinder edges, similar results are obtained in other planes transverse to the cylinder axis. These results are shown primarily to indicate the scale and relative magnitude of the high density region in front of the body. It is this increase in density that produces increased interaction between the

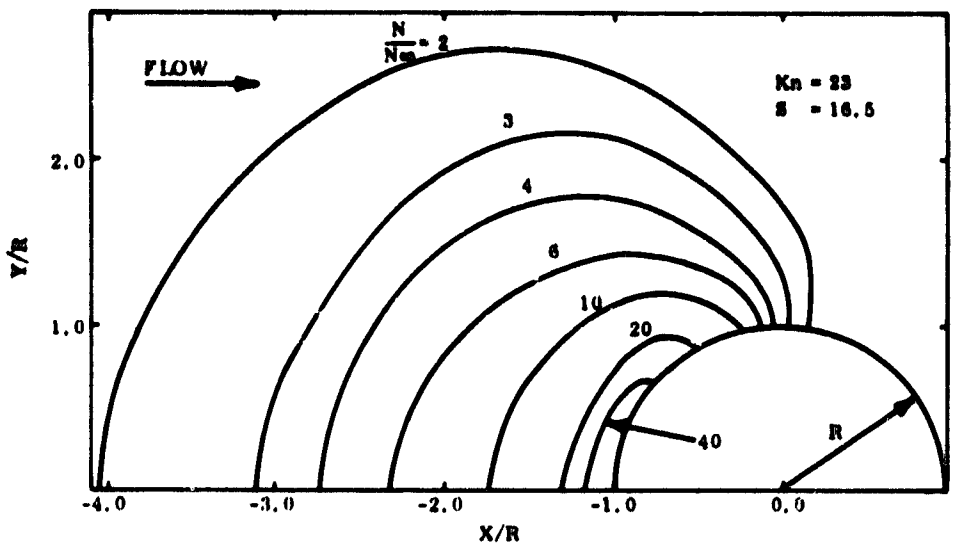

DENSITY CONTOURS FOR SHORT CYLINDER (L/R = 1.5)

a. Knudsen No. = 23

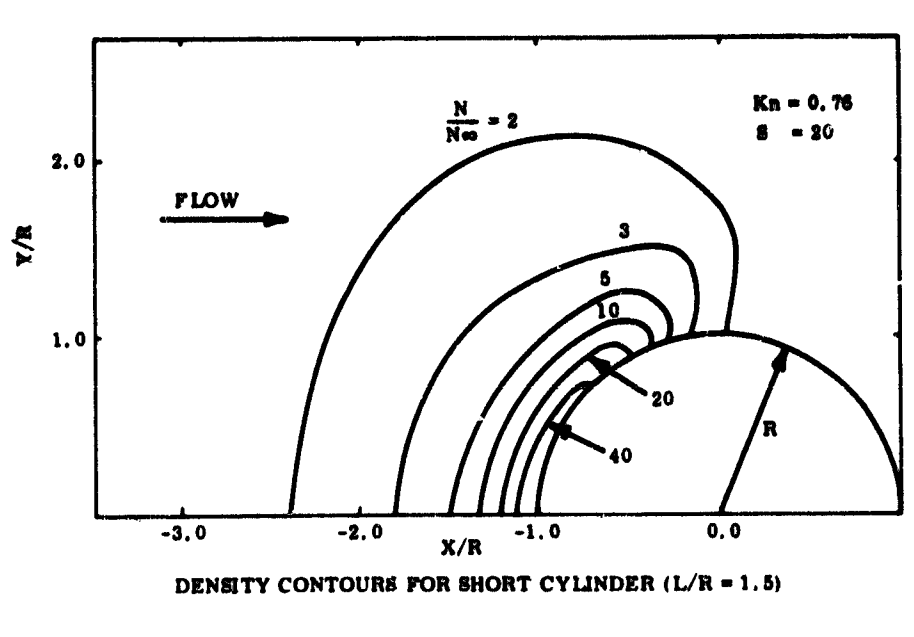

DENSITY CONTOURS FOR SHORT CYLINDER (L/R = 1.5)

b. Knudsen No. = 0.76

Figure 2. Density Contours for Flow About a Short Cylinder (Density Levels are Referenced to the Free-Stream)

particles and the body and thereby accounts for the rather pronounced effects at the surface even when the free-stream mean-free-path is considerably larger than the body (that is, at large Knudsen numbers). The compression of the high density region (measured in terms of the body dimensions) as Knudsen number decreases is also evident. Not noticeable on these figures, but readily apparent from the data, is the fact that the density immediately adjacent to the stagnation point also rises rapidly with decreasing Knudsen number. Figures 3a and 3b show similar results for a sphere (obtained from the two-dimensional programs developed for the previous contract). The physical

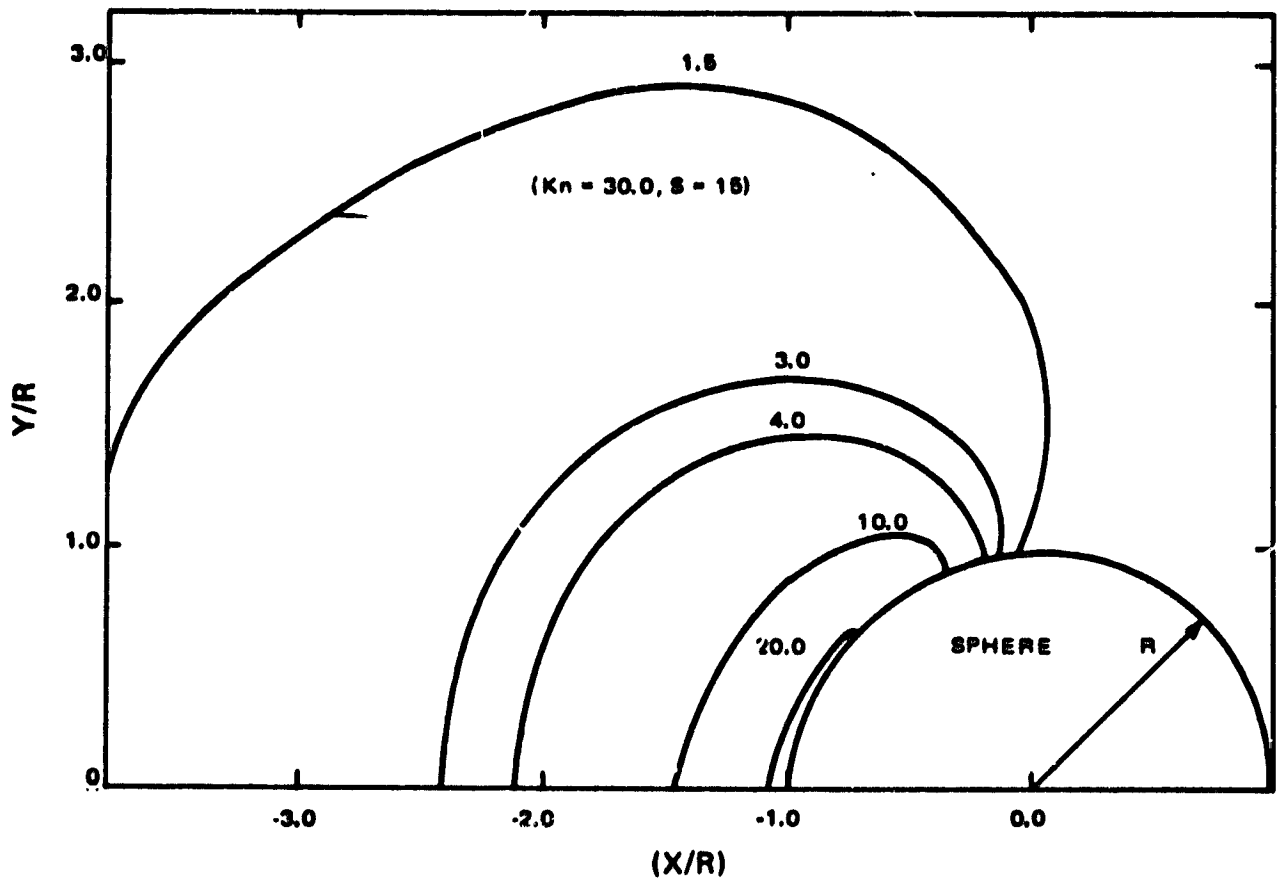

a. Knudsen No. is 30.0

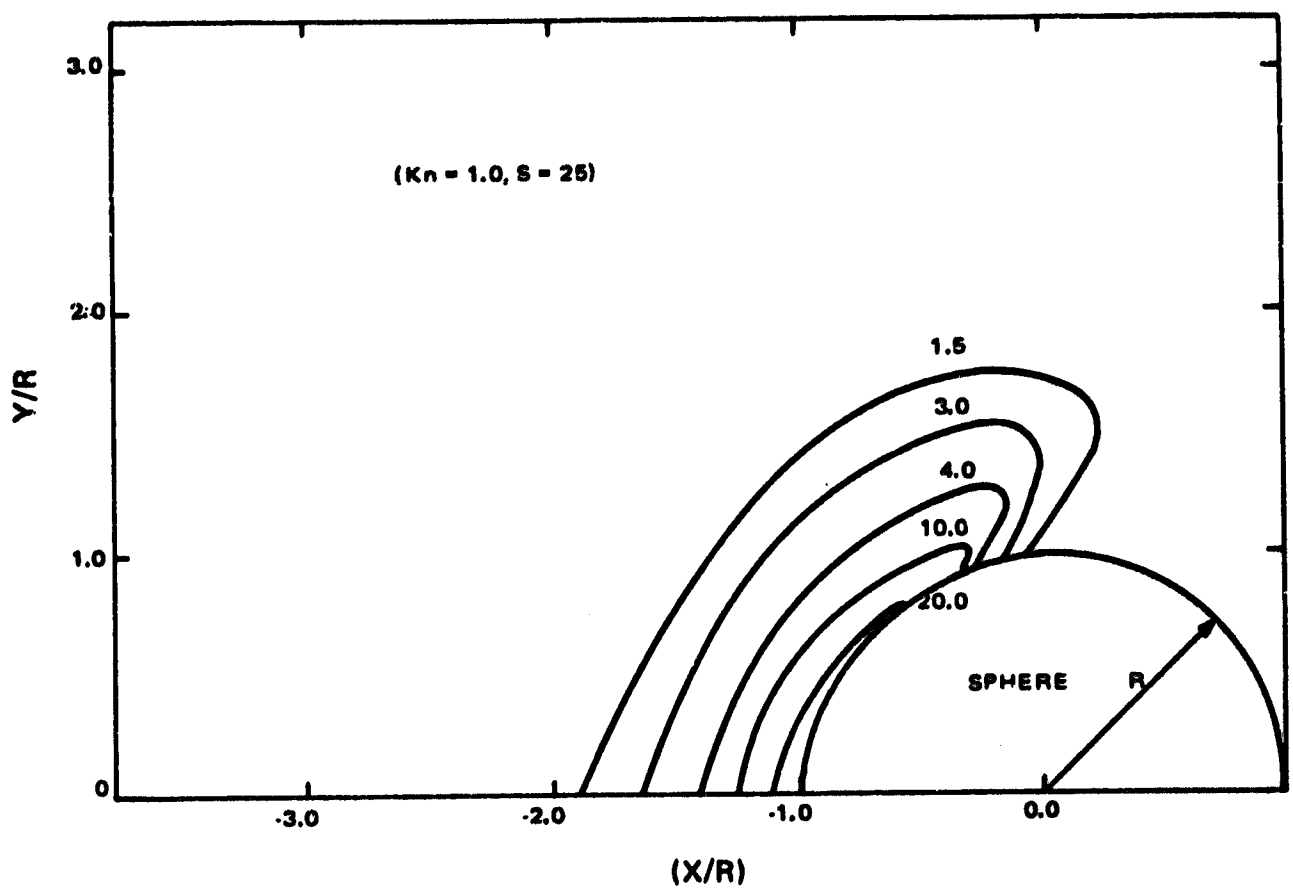

b. Knudsen No. is 1.0

Figure 3. Density Contours for Flow About a Sphere (Density Levels are Referenced to the Free-Stream)

parameters, other than geometry used as program inputs to obtain these figures were qualitively the same as those used to obtain Figures 2a and 2b respectively. The results are exactly as one would expect when considering the two geometries. In the spherical geometry, the body influence does not extend as far forward as in the cylindrical geometry, but qualitively, the features of the density contours are similar.

The kinetic temperature variation of the two species along the stagnation streamline (Z = 0) in the mid-plane for both a high (23) and low (0.76) Knudsen number is shown in Figure 4. At the higher Knudsen number, temperature is not a very meaningful quantity, as it arises simply from the superposition of the incoming and reflected distribution functions. The decay of the temperature to free-stream value takes place purely on the basis of the reduced solid angle subtended by the particles coming from the body. And, because the density of the reflected component is so high, this process extends many body diameters. At the lower Knudsen number, one sees the beginning of a shock layer. However, its extent and magnitude are very different from continuum results. In the continuum limit, the entire shock layer would extend no more than about twenty percent of a body diameter, while the peak temperature for both species would be 125 times the free-stream value. Note that for both species the extent is much larger while the peak temperature is lower. The differences between the light and heavy particle temperatures are in conformity with the qualitative results expected on the basis of incomplete collisional coupling between the two species.

A typical longitudinal variation of number flux per unit area, normalized to the free-stream flux,* at 5 degree and 45 degree azimuthal positions, and at a Knudsen number based on diameter Kn = 2.3, is shown in Figure 5. While generally, the number flux at the mid-plane is somewhat higher than that near the cylinder edges, the variation is no more than about 20 percent. Results for other Knudsen numbers are qualitatively similar. Because of limited spatial resolution, the present results cannot determine behavior very close to the cylinder edges and should not be used to infer that a local variation much more pronounced than that in Figure 5 does not exist.

Figures 6 through 14 show some selected azimuthal variations of number flux for a heavy and a light species of gas. Both values are normalized to the free-stream value (the free molecular value is also indicated on the plot as a means of comparison) and are plotted for several Knudsen numbers. In all cases the body surface was assumed cold (temperature approximately equal to the free-stream temperature) with perfectly accommodated diffuse reflection. Figures 6 through 10 are for an approximate mass ratio of constituents, RM, of 1.75

---

* The free-stream flux is the free-stream number density, N_∞, multiplied by the free-stream velocity, U_∞.

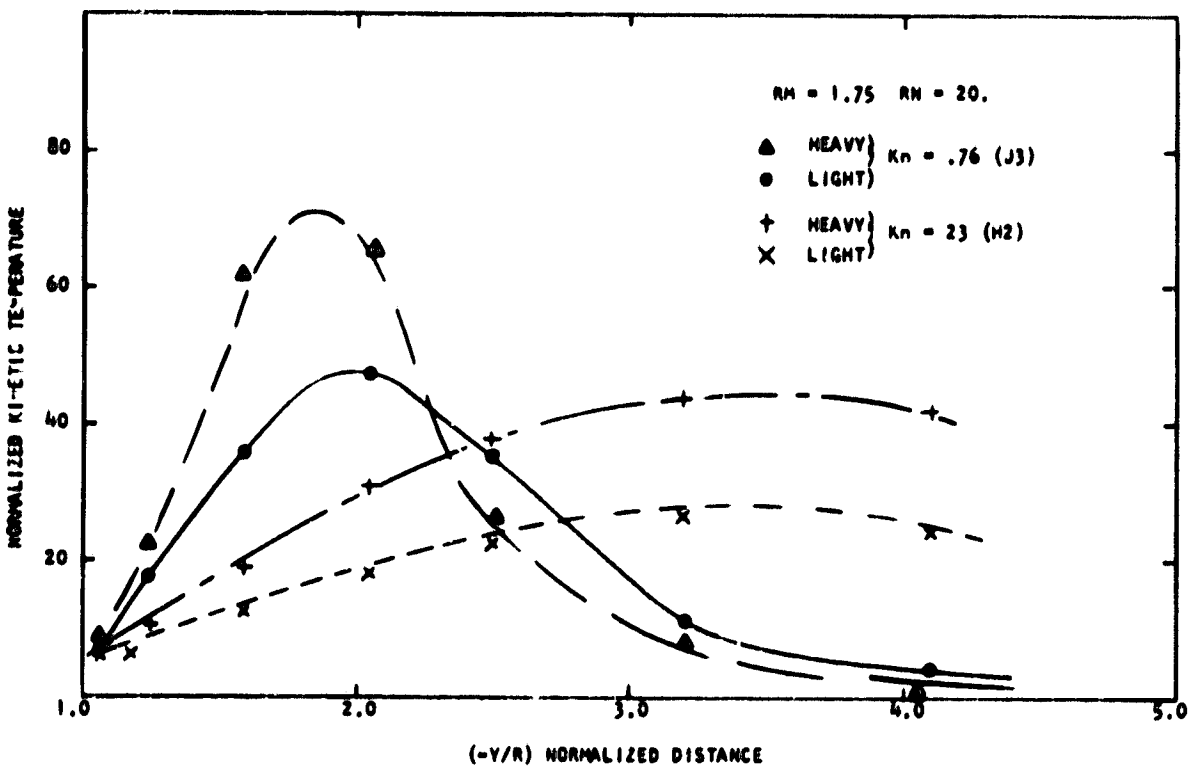

Figure 4. Kinetic Temperature Profiles Along the Stagnation Stream-Line in the Mid-Plane of a Short Cylinder

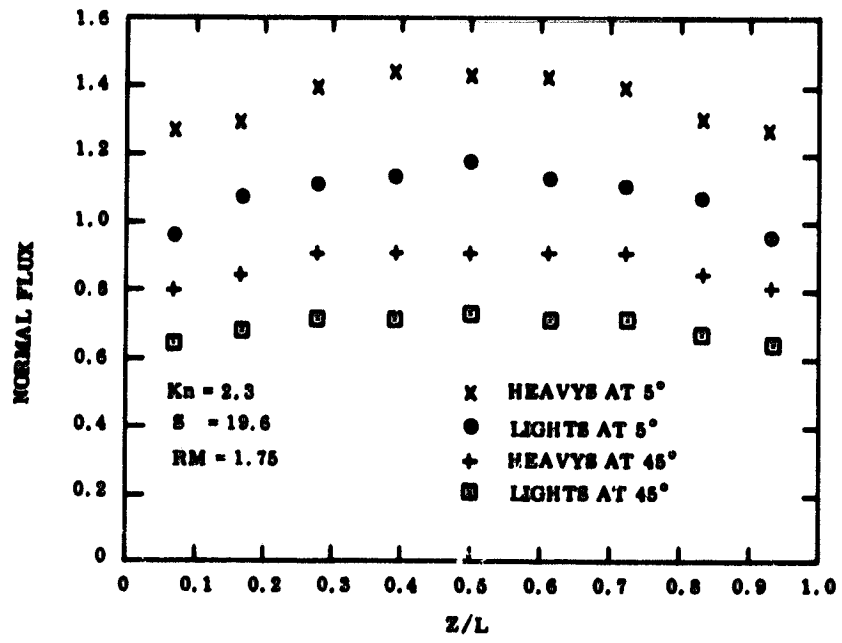

Figure 5. Longitudinal Variation of Normalized Number Fluxes Along a Short Cylinder Transverse to the Flow (Light Species is a Trace Constituent)

(N_2 to O ratio). The results presented are for free-stream concentration (number density) ratios, RN, of 7.7, 20 and 2.0. Figure 6 gives an indication that at a Kn of 23 the results, to within their accuracy, are free molecular. The consistently higher value for the heavy species suggests, however, that the collisional increase of surface flux is already apparent for the heavy species. Figures 7 and 8 correspond to lower Knudsen numbers (7.6 and 2.3 respectively) and show qualitatively similar azimuthal variation but at increased values of flux and greater separation between the species. Figures 9 and 10 are for a Knudsen number of 0.76 and for concentration ratios, RN, of 20 and 2.0 respectively. At this Knudsen number, the heavy species is eighty percent greater than the free molecular flux at the stagnation point, and the separation between the two species is very pronounced. Note that, while the heavy species flux varies only slightly between concentration ratios of 20 and 2.0, the light species flux is appreciably lower for the ratio-of-20 case. A similar flux profile for a Knudsen number of 0.76 and for an approximate mass ratio, RM, of 7.0 (N_2 to H_e) while RN is 20 is shown in Figure 11. The results here are very similar to those in Figure 9, indicating that when the light species is a trace constituent, the mass ratio is not an important parameter in determining the collisional increase of flux of either species.

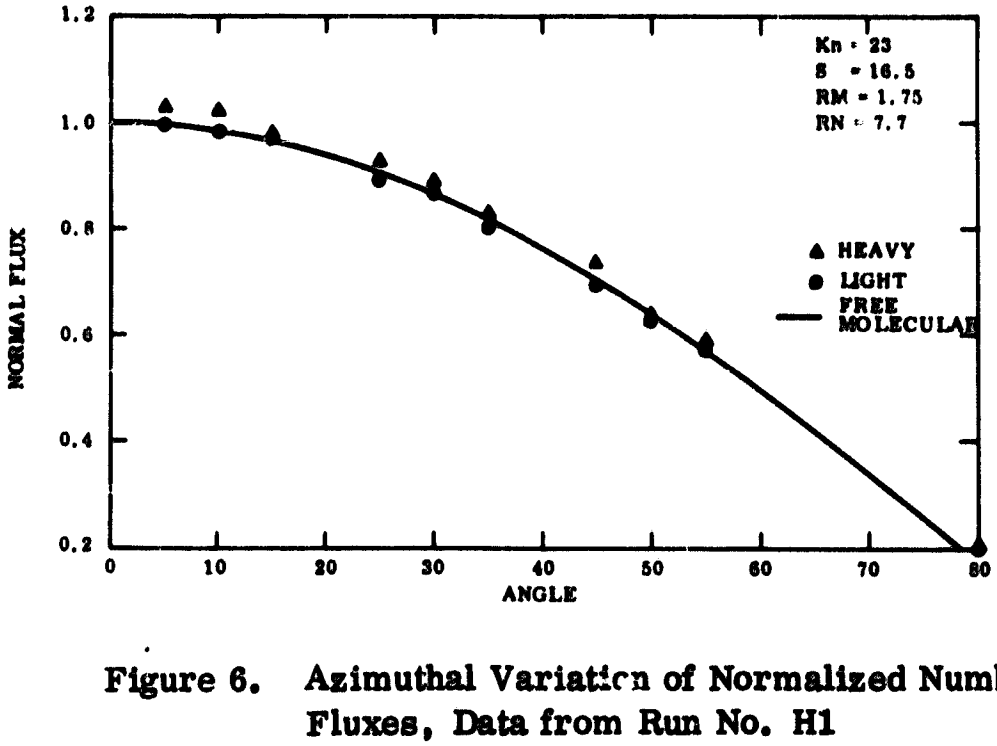

Figure 6. Azimuthal Variation of Normalized Number Fluxes, Data from Run No. H1

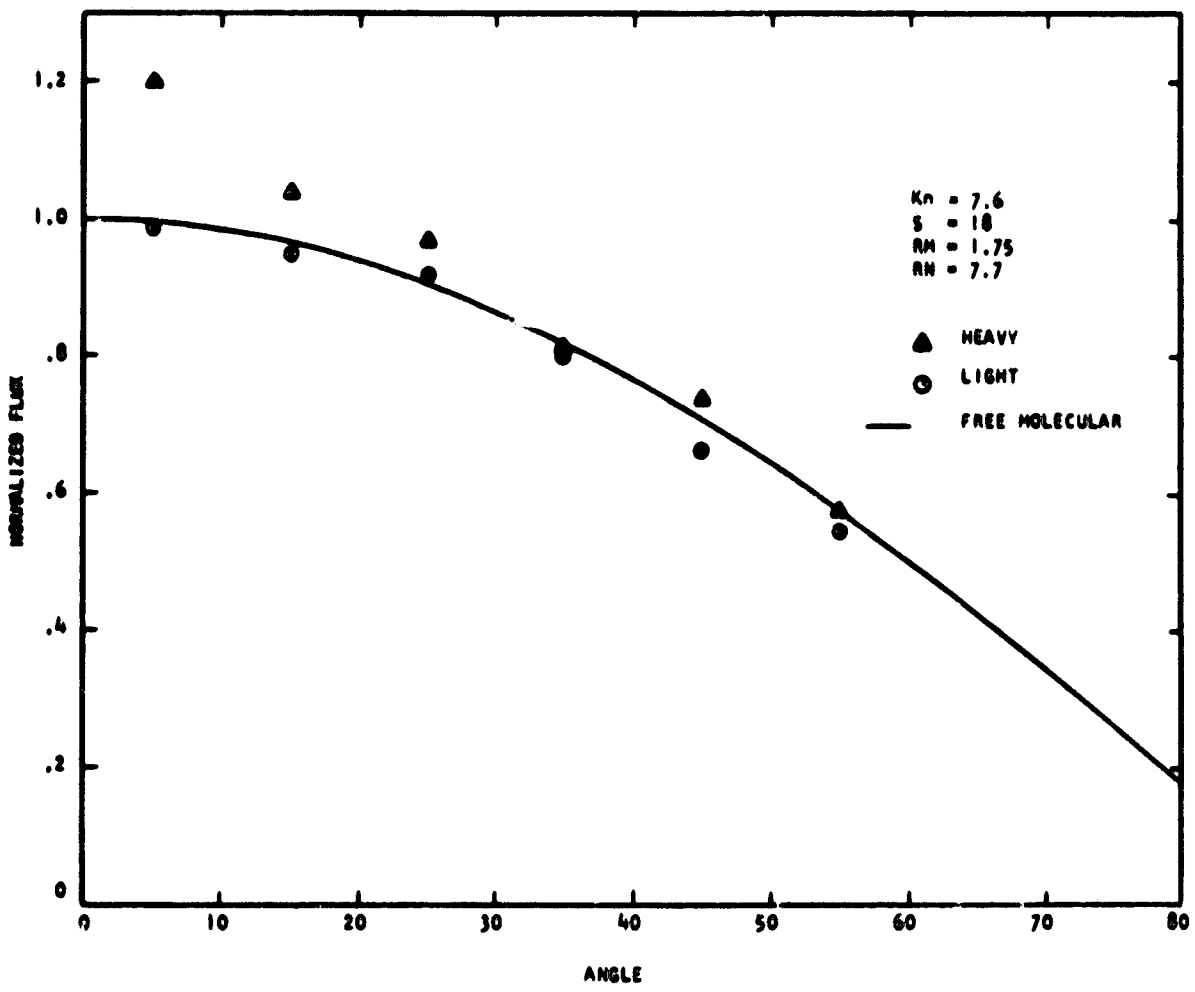

Figure 7. Azimuthal Variation of Normalized Number Fluxes, Data from Run No. M2

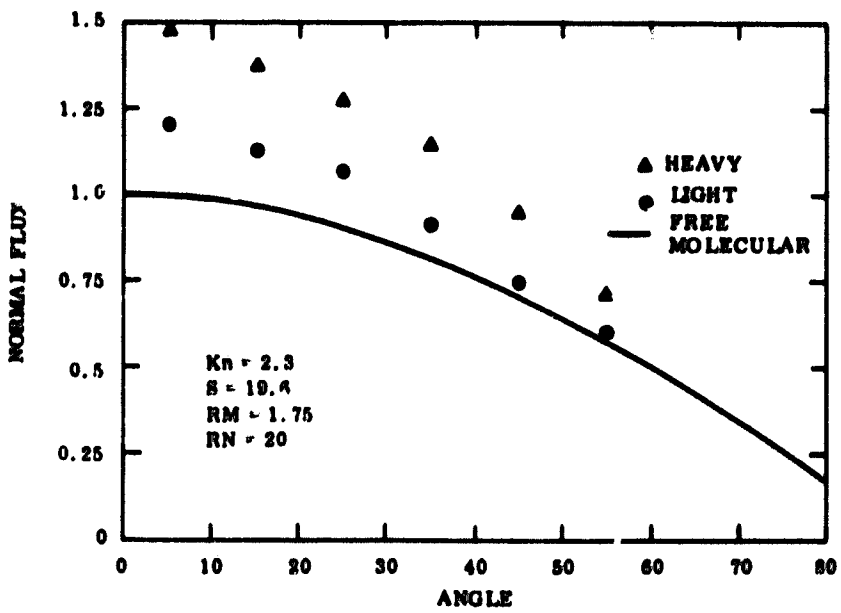

Figure 8. Azimuthal Variation of Normalized Number Fluxes, Data from Run No. L2

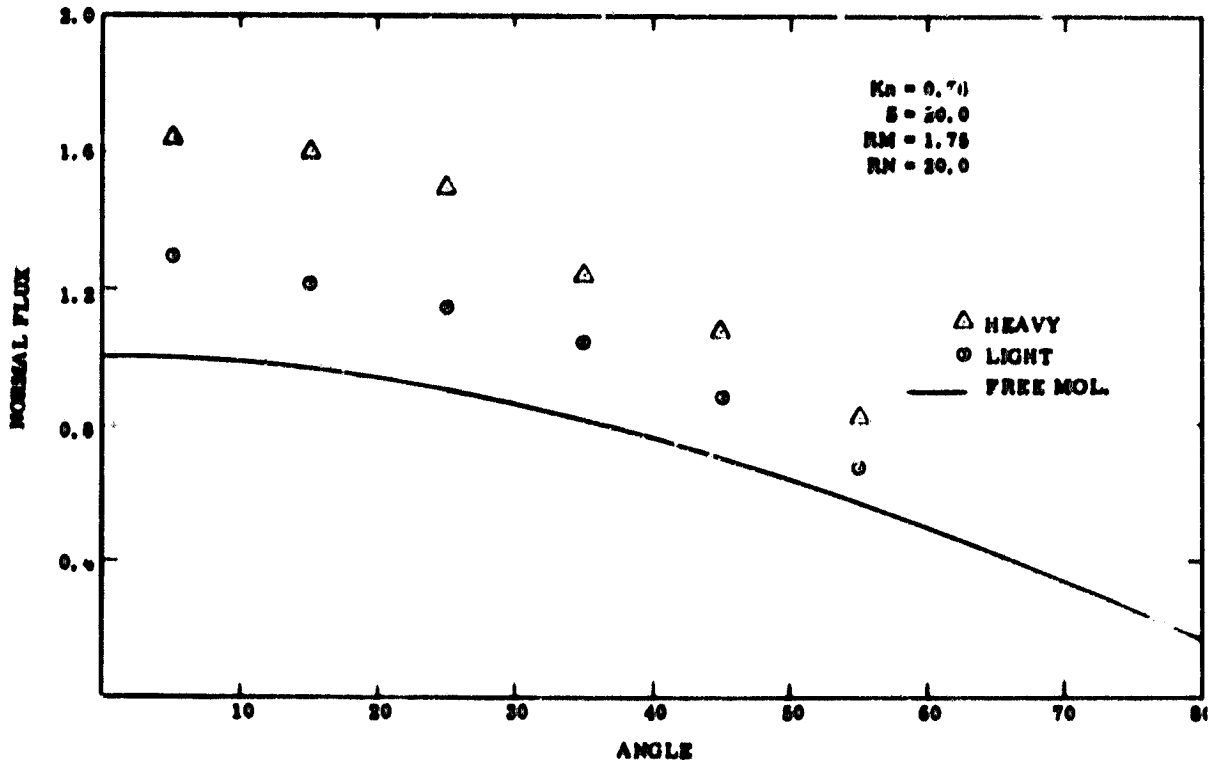

Figure 9. Azimuthal Variation of Normalized Number Fluxes, Data from Run No. J3

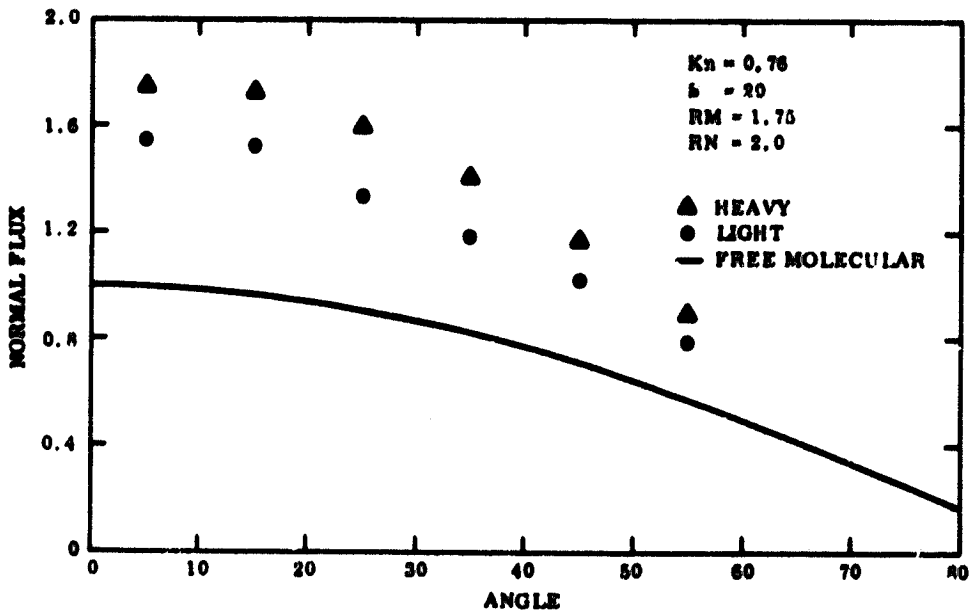

Figure 10. Azimuthal Variation of Normalized Number Fluxes, Data from Run No. J1

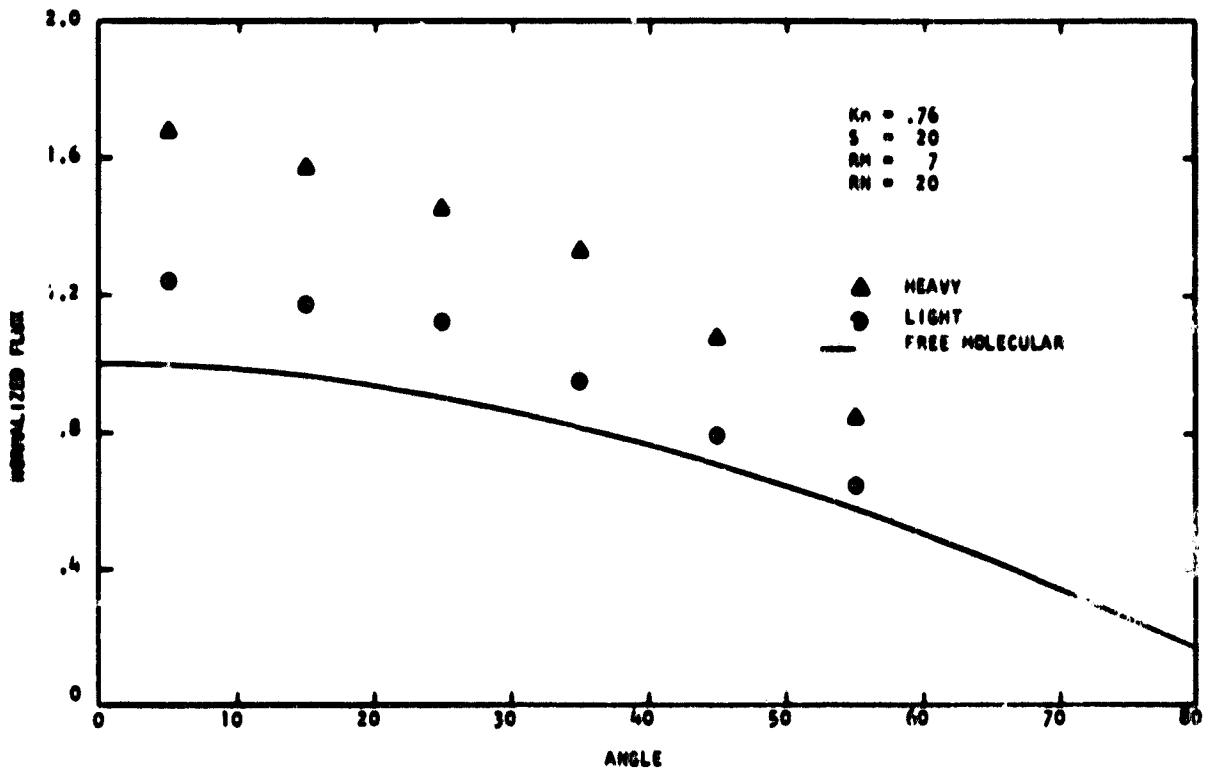

Figure 11. Azimuthal Variation of Normalized Number Fluxes, Data from Run No. J4

Figures 12 to 14 show the normalized azimuthal flux variation for a Knudsen number of 0.76, an approximate mass ratio of 0.875 (N_2 to O_2) and for concentration ratios of 2.0, 7.7, and 20.0 respectively. At an RN of 2.0, no pronounced separation (in excess of the accuracy) is clearly discernible, although a slight excess of flux exists for the more numerous light species. As the concentration ratio of the light to heavy species is increased, the light species flux is only slightly decreased while a very pronounced depletion of the heavy species flux appears at the stagnation point.

The relative species fluxes in Figures 13 and 14 appear to contradict the general trend of heavy species overabundance seen in the results from the other mass ratios (1.75 and 7.0) in Figures 6 to 11. However, qualitatively similar results were found at other Knudsen numbers. While no concrete explanation can be given, major differences between the cases can be indicated. All of the results for mass ratios of 1.75 and 7.0 represent situations where the heavy species is dominant in terms of momentum and energy content of the flow, and the light species has appreciably lower mass. The cases shown in Figures 13 and 14 represent the flow of a mixture of molecules of only slightly different masses and with momentum and energy carried primarily by the lighter species. Only additional computations and analysis in this range of mass and number density ratios can explain the reasons for the apparent light species overabundance.

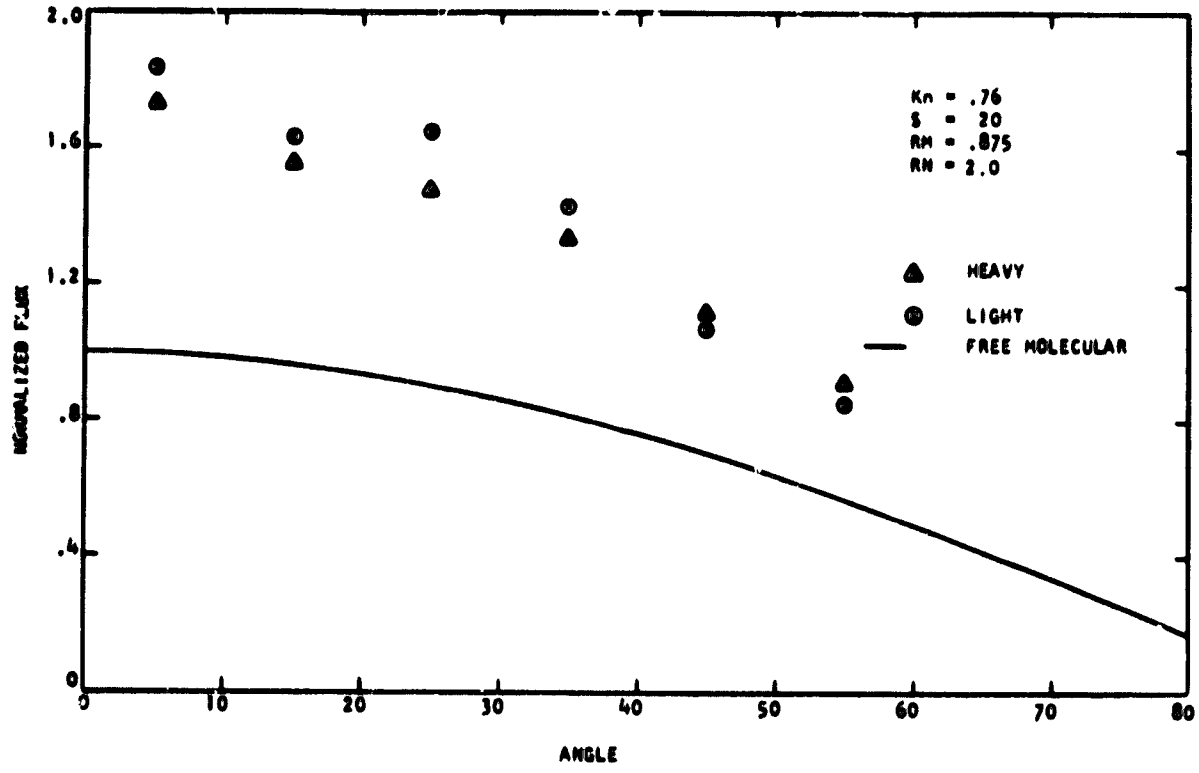

Figure 12. Azimuthal Variation of Normalized Number Fluxes, Data from Run J5

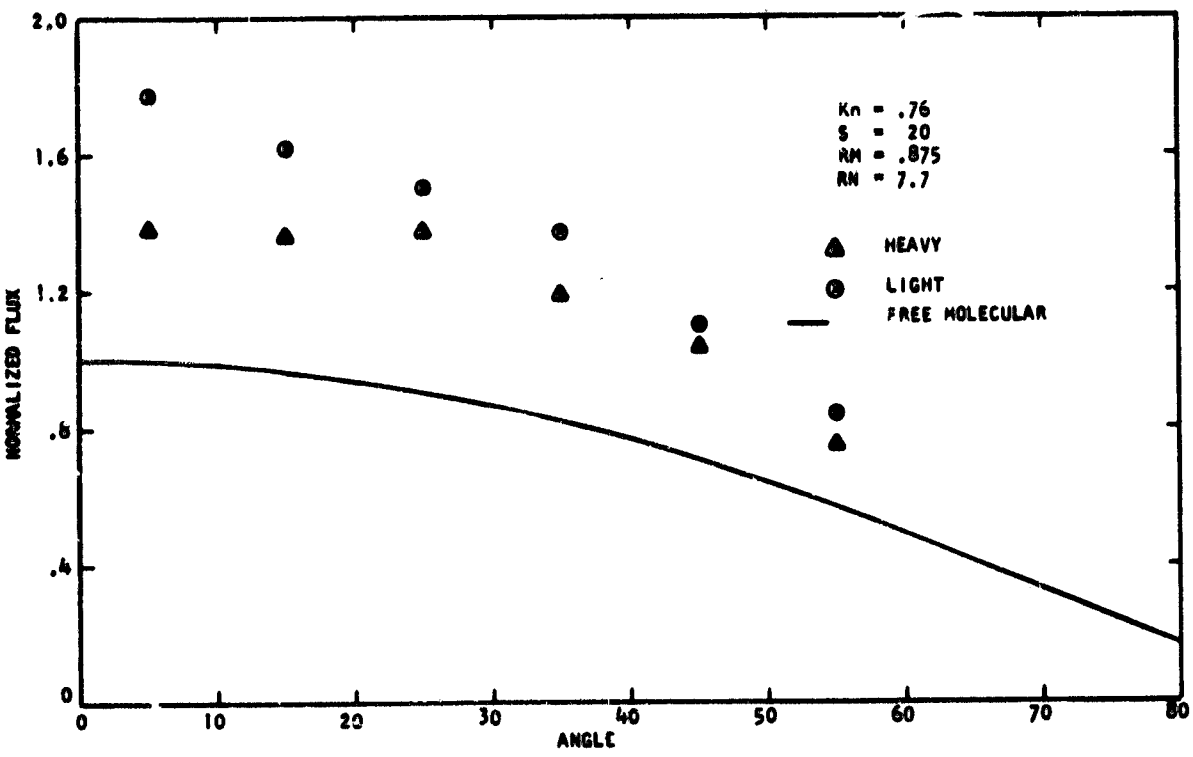

Figure 13. Azimuthal Variation of Normalized Number Fluxes, Data from Run No. J6

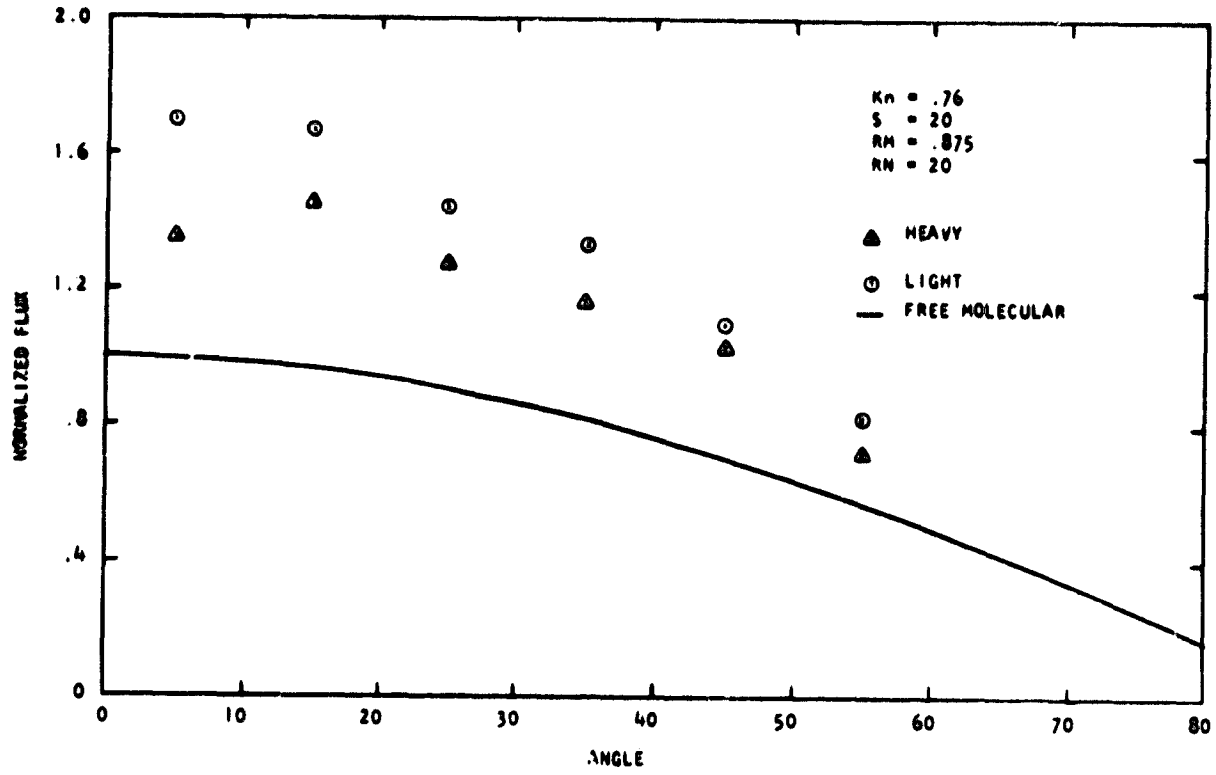

Figure 14. Azimuthal Variation of Normalized Number Fluxes, Data from Run No. J7

The azimuthal variations of pressure (normal stress) and shear in the mid-plane at a Knudsen number of 0.76 is shown in Figure 15. The pressure even at this relatively low Knudsen number is not very different from free molecular results. Simple momentum conservation requirements, together with the fact that free molecular and inviscid continuum stagnation point pressures are only a few percent different, tend to confirm the plausibility of this result. The shear coefficient, on the other hand does show a decrease of the order of 20 percent. (The shear coefficient must approach zero in the inviscid limit.) This slight reduction of shear suggests an even smaller reduction of drag coefficient. A similar plot of the heat transfer coefficient* at several Knudsen numbers is shown in Figure 16. From this figure it can be seen that the coefficient of the heat transfer term (or net energy flux to the surface) decreases

---

* The heat transfer coefficient may be expressed as:

$$\frac{q}{1/2\rho_\infty U_\infty^3}$$

where ρ_∞ is the free-stream mass ratio and U_∞ is the free-stream velocity.

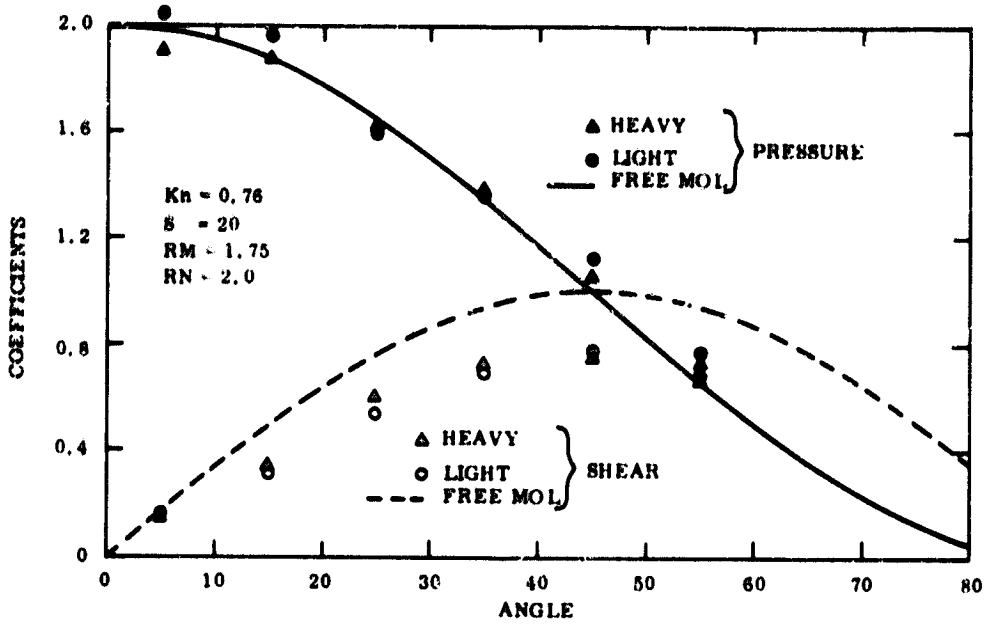

Figure 15. **Azimuthal Variation of Pressure and Shear Coefficients in the Mid-Plane of a Short Cylinder, Data from Run No. J1**

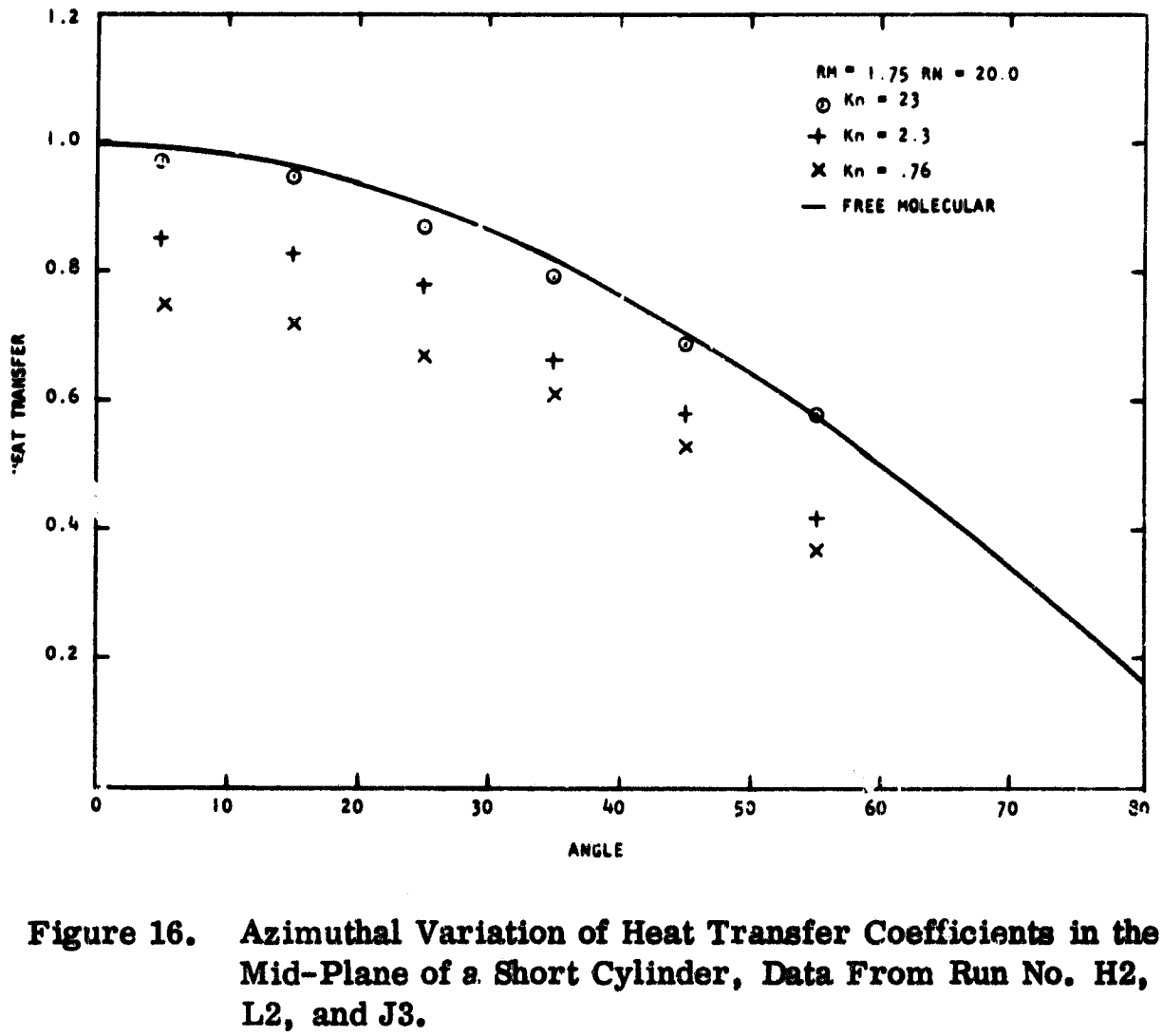

Figure 16. **Azimuthal Variation of Heat Transfer Coefficients in the Mid-Plane of a Short Cylinder, Data From Run No. H2, L2, and J3.**

with decreasing Knudsen number with reduction of approximately twenty-five percent at the stagnation point at a Knudsen number of 0.76.

The normalized flux results for a Kn of 0.76 at the stagnation point and a position 45 degrees from the stagnation point in the azimuthal direction are summarized in Figure 17. It shows the variation of the heavy to light flux ratio at the surface normalized to that in the free-stream as a function of concentration ratio and for several mass ratios. Figure 18 is a summary of the normalized flux results. It shows variation with Knudsen number for two concentration ratios (20 and 2.0) but for a constant mass ratio of 1.75. Note that for Knudsen numbers of 2.3 and higher, almost no effect of concentration ratio is discernible, while at a Kn of 0.76 the results show a pronounced difference which could be expected from comparing Figures 9 and 10.

Aside from the direct effect of increased flux entering an instrument orifice, the form of the distribution function can have very serious consequences on the calibration of such an instrument. It is well known that even if the internal flow connecting the orifice and the measuring instrument is free molecular, the relation between internal pressure and the entering flux is very sensitive to the form of the distribution function[9]. When the external flow is in the transitional flow regime the input distribution function at an orifice must be composed of two separate distribution functions from the two classes of particles: (1) the "uncollided" particles, coming directly from the free-stream, and (2) the "interacted" particles, coming from products of collisions between the free-stream molecules and either the "body reflected" or the "interacted" molecules coming away from the body. As explained in Section III, at preselected locations the distribution functions of both collided and uncollided molecules can be monitored. A typical result which has been "polynomial-fitted" for use in the internal flow program is shown in Figure 19. The first and third rows of graphs represent curves directly fitted to the data (which comes as a list of values designating the fractional number of surface collisions at that segment with velocities below a specified tabulated velocity). Rows 2 and 4 show the derivatives of the fitted curves and represent the distribution functions of the molecules. Rows 1 and 2 give the free-stream molecules' curves while rows 3 and 4 give similar curves for the interacted molecules. Each function is divided into three Cartesian Coordinates, normal, azimuthal and longitudinal, in directions with respect to the body surface and flow direction. Note that the uncollided molecules are peaked around a high incoming velocity with a spread of a few times the thermal speed as expected. The collided moelcules in turn have a broad distribution, in general with a spread more representative of the vehicle speed. As can be seen from the figure, should a spacecraft-borne instrument be a priori calibrated assuming a very peaked flux distribution function, an appreciable portion of the collided molecules could greatly alter the calibration, thereby producing erroneous results.

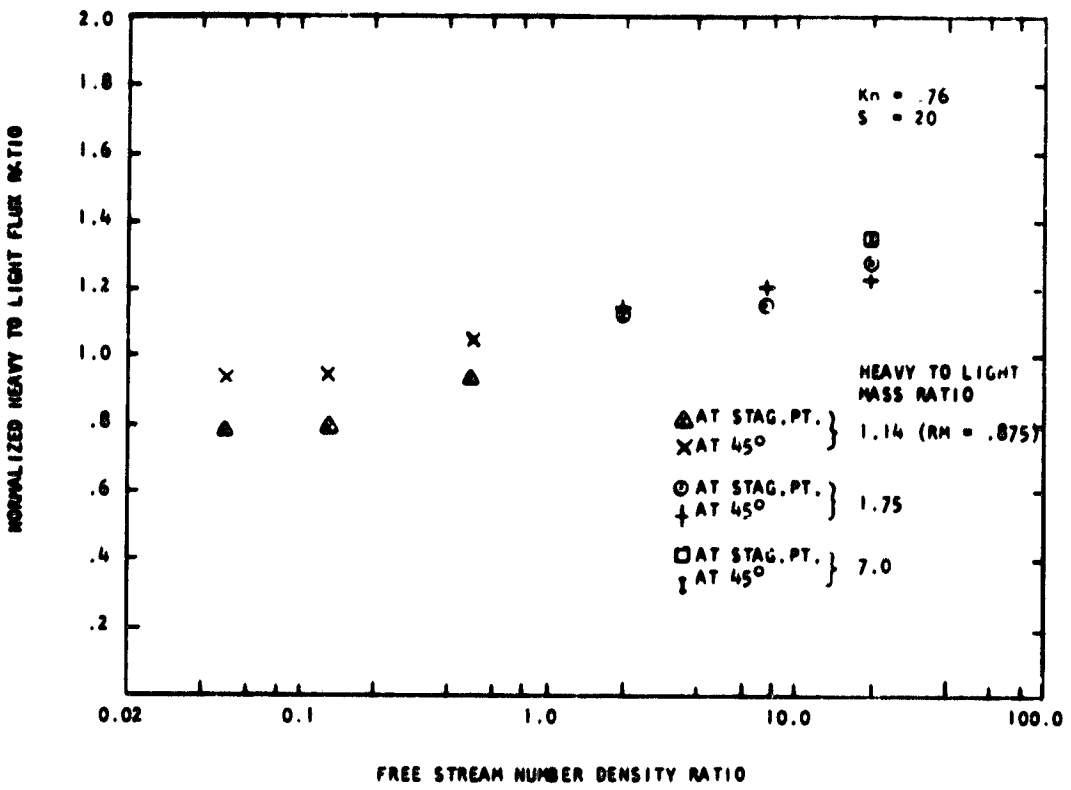

Figure 17. Variation of Normalized Flux Ratio with Free-Stream Number Density Ratio

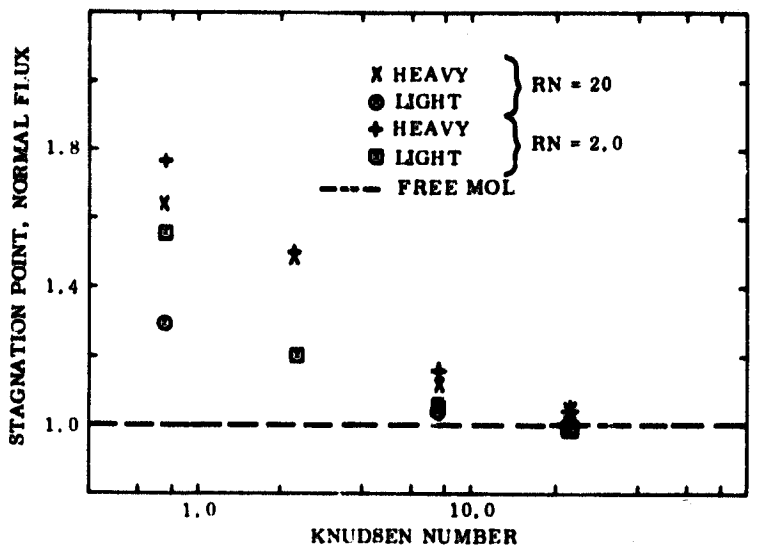

Figure 18. Stagnation Point Flux Variation with Knudsen Number for a Short Cylinder Mass Ratio is 1.75

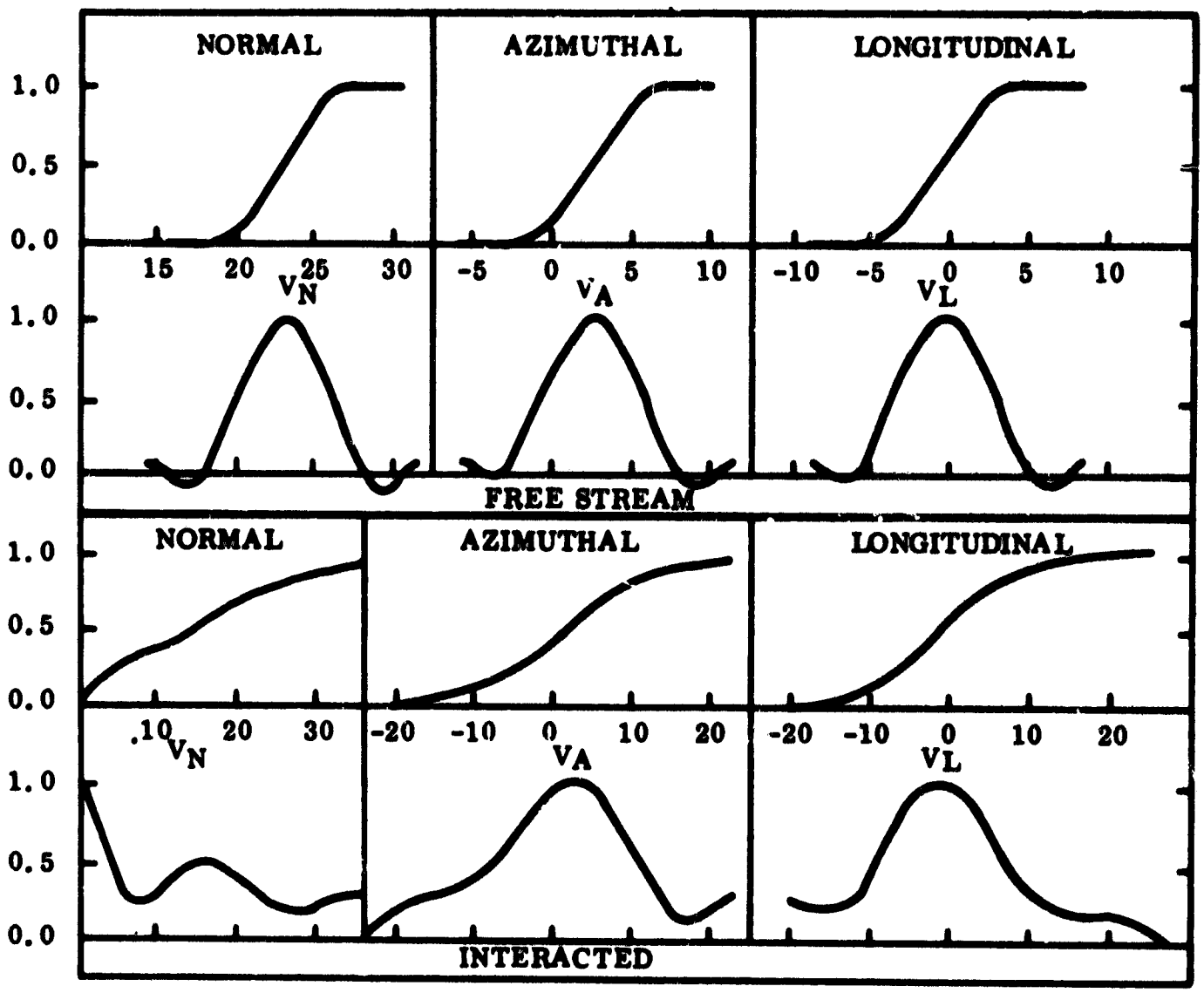

Figure 19. Fitted Distribution Functions at 5 Degree Azimuthal Surface Position in the Mid-Plane of a Short Cylinder

The variation with Knudsen number of the uncollided fraction of the incoming flux at the stagnation point in the mid-plane is shown in Figures 20 and 21. In Figure 20, two mass ratios are shown for the case in which the light species is a trace constituent and in Figure 21 the effect of varying concentration ratio and surface location is shown for the mass ratio of 0.875. Note that, in all cases, for Knudsen numbers near one a large fraction of the flux comes from collided molecules having a distribution in no way resembling the free-stream particles. Thus instrument calibration based on the highly directed molecular beams available in the laboratory may be of little value.

Some indication of the variation of several parameters as a function of Mach number is given in Figure 22. A word of caution is necessary here to prevent misinterpretation. The important parameter is really not the Mach number based on the free-stream speed of sound. It is the Mach number based on a sound speed based on body temperature that is relevant. Note that such a Mach number, squared, represents a ratio of incoming kinetic energy to the energy of the outgoing particles. As long as the free stream Mach number is relatively large ($S > 5$), the free-stream temperature can be shown to play essentially no role, at least on the forward portion of the body. The variation with Mach number for this figure was essentially obtained by keeping the body temperature equal to the free-stream temperature and thus varying the "body Mach number", (which is, in actuality, the relevant quantity) simultaneously with the free-stream Mach number. The results shown are for the relatively high Knudsen number of 7.6. The surface flux does not show a pronounced change, but the fraction of uncollided particles reaching the surface is definitely reduced for increased Mach numbers. This is at least partially explainable by looking at the increasing number densities in the "cell" immediately in front of the body segment on which the collisions are being monitored.

Figure 23 represents an attempt to obtain some knowledge of variation of surface fluxes with body geometry from the very limited information gained thus far. This figure is a summary of results of the stagnation point flux on a sphere, an infinite cylinder and the short cylinder ($L/R = 1.5$) discussed in this section. The plot is for a large mass ratio ($RM \geq 7$) and the light species is again a trace constituent. The upper portion of the figure shows total flux (primarily heavy particles) as a function of Knudsen number. Although there are some differences between the three geometries, no pronounced trend is discernible. The lower portion of the figure shows the heavy-to-light flux ratio normalized by the free-stream value. There appears to be a definite trend, showing increasing heavy species overabundance as one proceeds from the spherical through the short cylinder to the pure two-dimensional, infinite-transverse cylinder geometry.

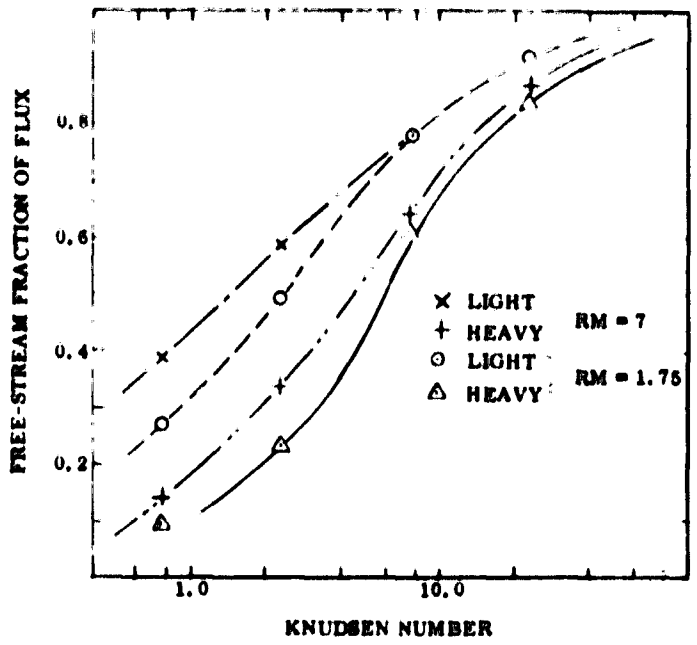

Figure 20. Variation of Free-Stream Fraction of Stagnation Point Number Fluxes with Knudsen Number (Light Species is a Trace Constituent)

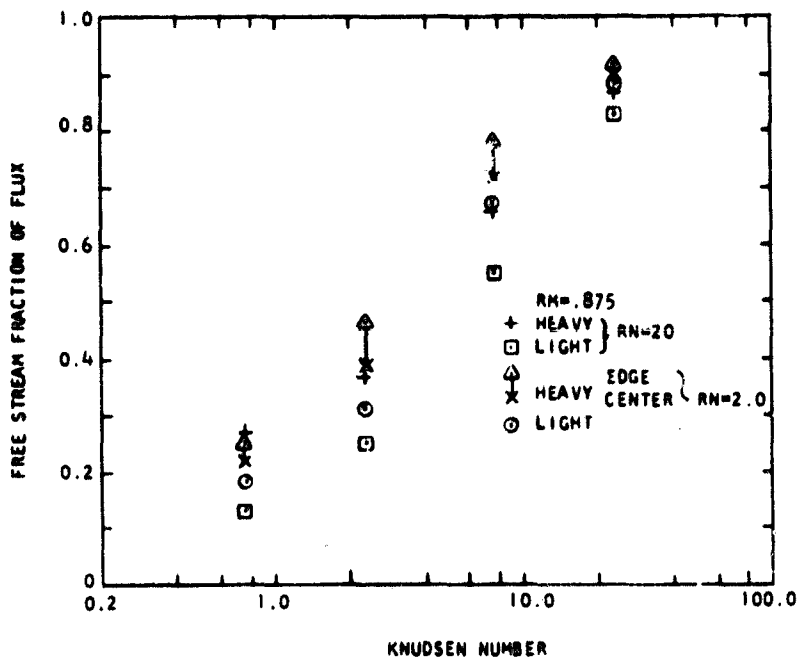

Figure 21. Variation of Free-Stream Fraction of Stagnation Point Number Fluxes with Knudsen Number (Mass Ratio is 0.875)

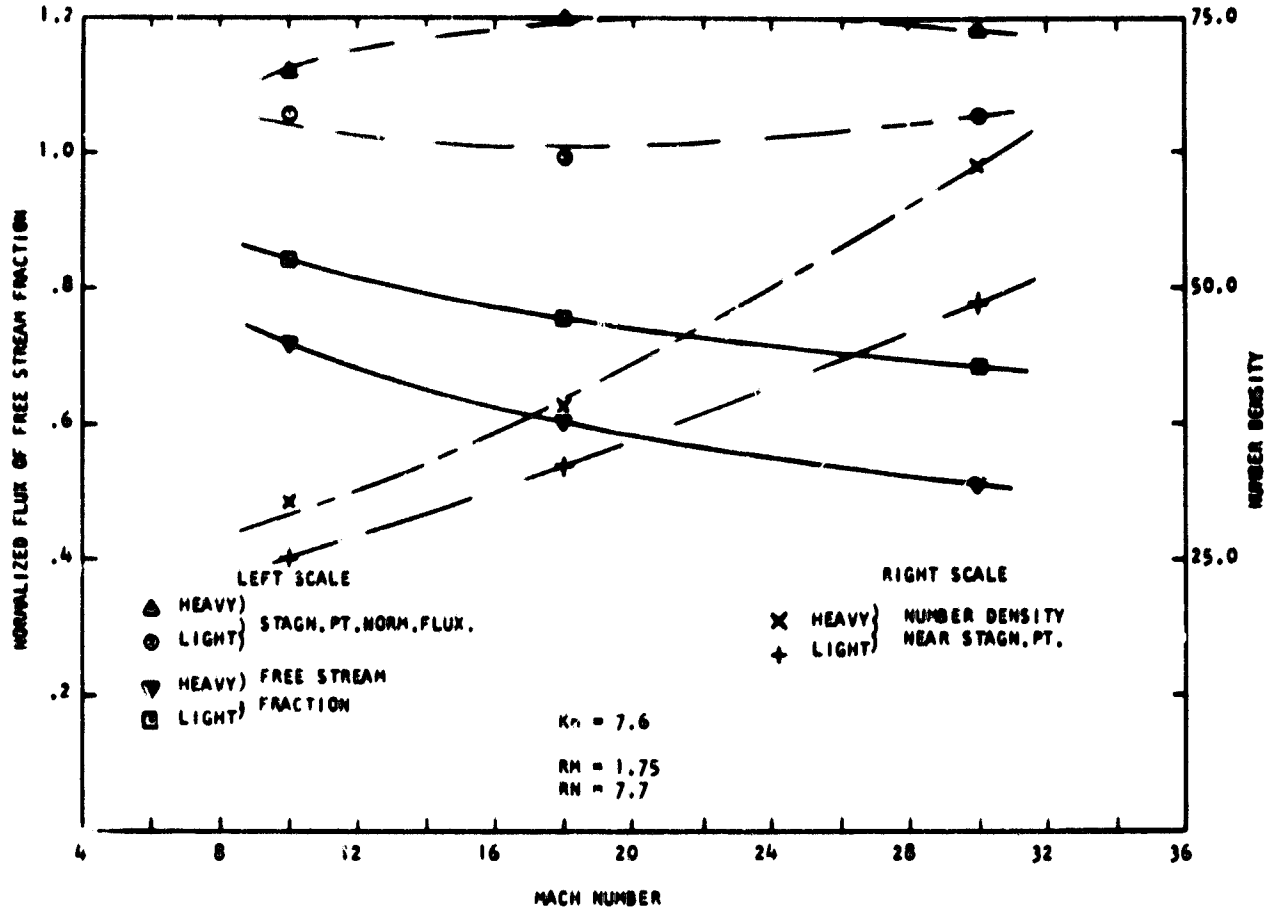

Figure 22. Variation of Stagnation Point Conditions with Mach Number of the Flow, Data is from Run No. M2, M8, and M9

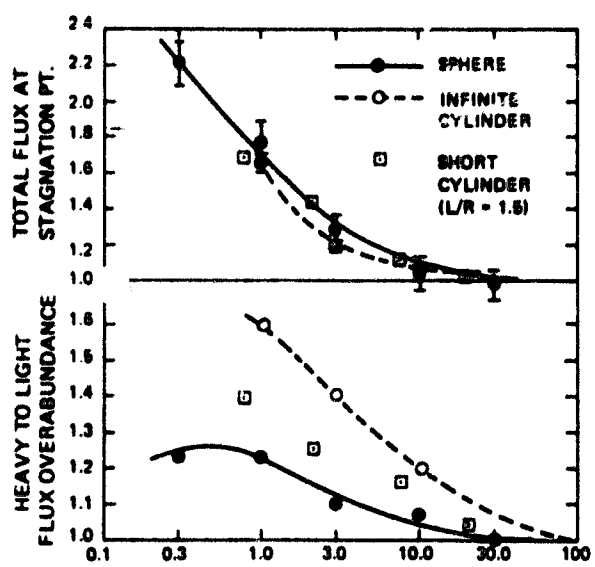

Figure 23. Variation of Flux at the Stagnation Point with Knudsen Number for Three Geometric Shapes

2. Results Obtained From The Internal-Flow Program

To test the operation of the internal-flow computer program in its revised form and to obtain some experience with the conditions expected in an instrument cavity on a vehicle under conditions computed in the external flow program, four "internal" runs were completed. Runs I1 and I2 used input distribution functions from the external flow run J4 (see Table 1) at the 5-degree azimuth location near the cylinder edge and in the mid-plane respectively. Runs I3 and I4 used input distribution functions from the 5-degree azimuth location in the mid-plane and are taken from external flow runs L4 and M4, respectively (see Table 1).

In all four runs, the instrument cavity geometry used was the same. The geometry chosen was a model of a long cylindrical tube preceeded by a short cylindrical constriction at the entrance, the short constriction leading from the orifice to the cylinder. A sketch of the section through the axis of symmetry of the geometric configuration used is shown in Figure 24a. The diameter of the constriction (called the "Entrance Region" on Figure 24a) is approximately 2 inches for a vehicle length near 50 inches while the diameter of the tube portion (called "Cavity Region") is twice as large (i.e., 4 inches). Figure 24a gives the dimensions in free-stream mean-free-paths for runs I1 and I2. The corresponding dimensions for I3 and I4 can be obtained by dividing the scale by 3 and 10 respectively. Figure 24b shows the variation of surface number fluxes normalized by the free stream value ($N_\infty U_\infty$) for each species for runs I2 and I3. No attempt was made to compute the azimuthal variation. This is because the angle between the perpendicular to the orifice and the flow direction is only five degrees. This low internal "angle of attack" implies only a very small amount of asymmetry of the entering distribution function and thus a small azimuthal variation within the cavity. The running times were insufficient to produce adequate statistics for detecting this variation.

Because of the limited number of runs of the internal flow program obtained thus far, only preliminary identification of the major effect can be attempted. In Figure 24b, the values of the normalized flux at 0.0 on the x-axis correspond directly to the flux per unit area entering the orifice (computed in external flow). The surface flux within the entrance region is somewhat lower than that entering the orifice. This conforms to the expectation that a large fraction of these particles can pass through the entrance region without collisions with the walls. Beyond the entrance region, the surface flux is generally higher than that at the orifice, with the effect more pronounced near the end of the cavity for the heavy species, and more pronounced at lower altitudes (notice Run I2).

While the number densities in the cavity are not shown, the trends are similar to those for the surface fluxes. For example, immediately behind the entrance region the light and heavy densities for Run 12 are, respectively, about 23 and 61 times their free-stream values (i.e., comparable to the 24.6 and 64.8 theoretically expected values behind a thin orifice). The densities rise monotonically with X, similar to the surface flux rise shown in Figure 24. Near the end wall of the cavity the corresponding densities are 38 and 207 times their free-stream values.

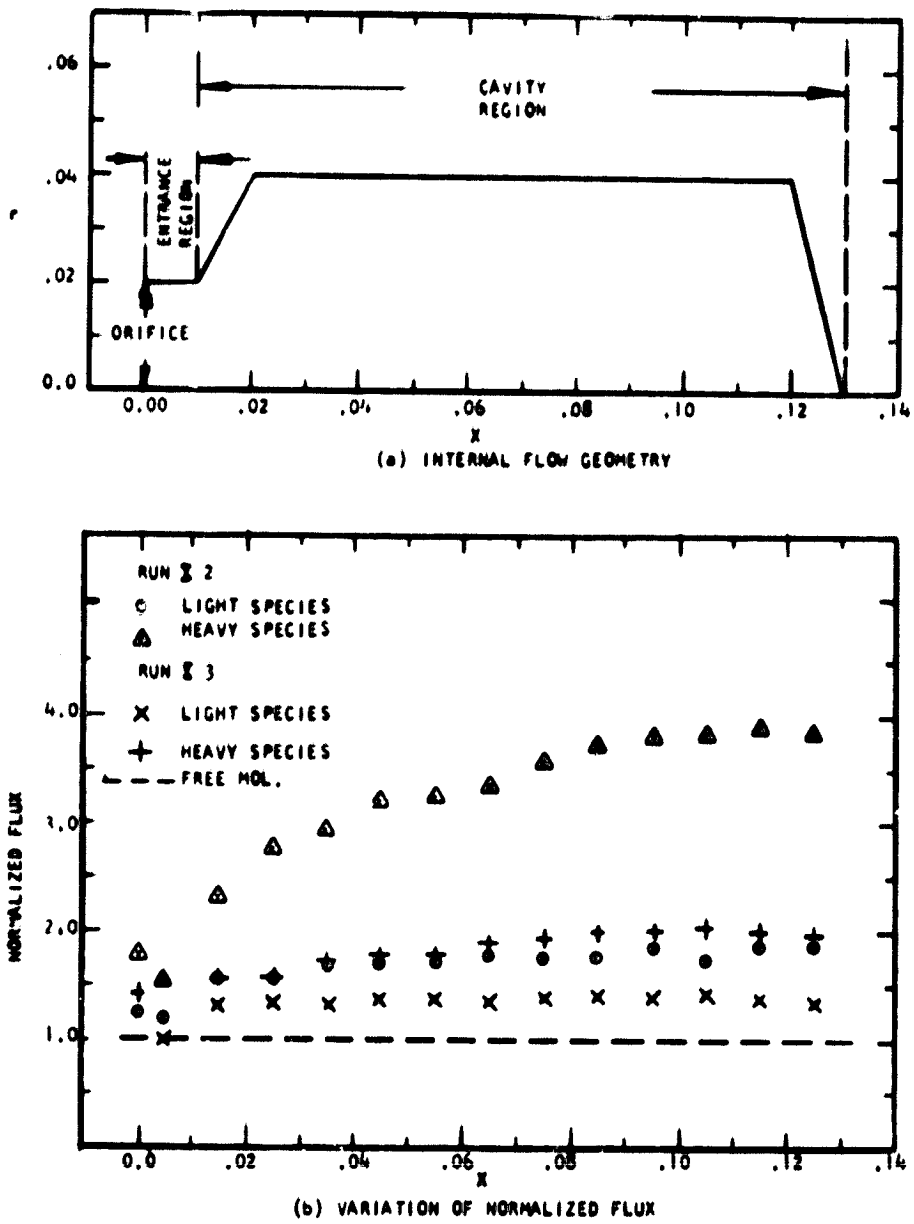

Figure 24. Internal Flow Results

The rise in flux toward the end of the cavity may be explanable on the basis of particle-particle collisions. Collision-dominated (continuum) theory predicts the normalized surface flux within the cavity of the heavy and light species for these runs at 10.3 and 3.9 respectively. Although, even for the I2 run, the results are not nearly this high, the effect of collisions is apparently significant near the cavity end. For free-molecular flow entering an extremely short entrance region and followed by large cavity in which the gas is in equilibrium with the walls (the classic example), the normalized surface flux for both species would be 1.0 everywhere within the cavity. This result is shown, for comparison, in Figure 24b and labeled "free-molecular."

D. THE THREE-FLUID PROGRAM

The necessity of treating three distinct fluids simultaneously is strongly coupled to the desire to include vehicle induced dissociation and possible chemical reactions. Since these tasks are beyond the scope of the current work and since most three-species gases are treatable with the existing program (see Section II, Para. D), no attempt was made to modify the current version of the programs. While the procedure for performing this modification is trivial in concept, it is very tedious in practice and requires extreme care in programming in order not to omit any of the necessary changes.

However, it is possible to estimate the expected increase in storage and computation times required by the addition of the third species. Going from a two- to a three-species gas mixture involves increasing the total number of particles by approximately 50 percent. Therefore, about a 40 percent increase in storage requirement can be predicted by increasing by 50 percent all species-related parameters in the program and increasing by 10 percent the length of the program itself. Because of additional experience with the external-flow, three-dimensional program, a somewhat more refined prediction of computational times than that attempted from the two-dimensional program can now be performed. A typical cycle time for once around the computational loop (which takes about 3 seconds in the present program) can be divided into three separate operations:

1. Calculating particle-particle collisions in subroutine COLLIDE,
2. Advancement of particle positions in subroutine MOVE, and
3. Bookkeeping operations involving updating of cell related properties in MAIN.

The time required for Operations 2 and 3 scales directly with the number of particles involved and thus a 50 percent increase for a third species would be expected. Time required for the operations in COLLIDE should scale with the number of particles squared and thus necessitate a 125 percent increase for the third species. In the current program, COLLIDE accounts for anywhere from a very small fraction of the total cycle time at high Knudsen numbers to approximately 1/3 the cycle time at low Knudsen numbers. On the basis of these estimates, one can expect the three-fluid program to require about a 50 to 75 percent increase in computational time along with the 40 percent increase in storage. Based on the current experience of 600 kilobytes and 50 to 60 minute runs, a three-fluid program is marginally feasible on the 360-91 Computer and definitely within the capability of the 360-95 Computer.

SECTION V

CONCLUSIONS

An operational, three-dimensional version of the external-flow two-fluid, direct-simulation, Monte-Carlo computer program has been developed. It is capable of generating the information necessary for vehicle design and for the location of flight instruments for measuring atmospheric properties in the altitude regime from 90 to 150 kilometers. The internal-flow program developed under the previous contract has been generalized so that it accepts as inputs information directly obtainable from the external-flow program. This capability should be of great value in instrument design and future data reduction.

The extensive number of cases run for the Atmosphere Explorer geometry using both the external- and internal-flow programs, together with the results from the previous contracts, have generated appreciable information on a number of phenomena expected to affect measurement of atmospheric properties in the lower thermosphere. The major affects are discussed below.

A. FLUX INCREASE AT THE STAGNATION POINT

The flux of particles per unit area at the stagnation point or, to a lesser extent, on any element on the forward portion of a vehicle increases rapidly with decreasing Knudsen number (for a fixed-vehicle geometry, decreasing Knudsen number corresponds to decreasing altitude). At a Knudsen number near one (corresponding to an altitude of about 110 kilometers), and using a vehicle having the Atmosphere Explorer geometry this increase approaches 100 percent.

The limited experience with different geometries (a short cylinder corresponding to the Atmosphere Explorer configuration, an infinite cylinder transverse to the flow, and a sphere) suggests that when the heavy species is dominant, the rise in flux of that species is not strongly affected by geometry. This trend is indicated in Figure 23.

B. DECREASE OF FREE-STREAM FLUX FRACTION AS ALTITUDE DECREASES

A result of great significance to the calibration of any instrument that will operate in the transition flow regime has been obtained. This is the computation of the extremely large reduction, with decreasing altitude, of the fraction of molecules arriving unperturbed at the surface of the vehicle. These results, presented in Figures 20 and 21, suggest that great caution be used in the interpretation of any results from an instrument designed and calibrated for a highly

peaked, free-stream distribution. As can be seen from Figure 19, if any appreciable number of particles are of the interacted type, the incoming distribution function will be very broad, with particles reaching the instrument entrance with almost equal probability from all directions.

C. OVERABUNDANCE OF HEAVY PARTICLE FLUX

It has been consistently found that whenever the heavy species is a major constituent, the flux increase of the heavy particles on the forward portion of the vehicle is appreciably more pronounced than for the light particles. This heavy species over-abundance appears to be strongly geometry-dependent on the basis of the cases considered in Section V, Para. A, and presented in Figure 23. For Atmosphere Explorer geometry, the expected measured helium mole factor would be about 40 percent too low and the atomic oxygen mole fraction 28 percent too low at an altitude of about 110 kilometers.

D. EFFECTS OF MACH NUMBER

The variation of Mach number (or speed ratio) has only a slight effect on the number fluxes on the forward portion of the body. A change of Mach number produces a much more pronounced effect on the fraction of those molecules colliding with the surface that had arrived previously unperturbed by the presence of the body. It is important to note that the relevant parameter in high-speed flow is the Mach number based on the body temperature, and not on the free-stream gas temperature. Thus, in a situation where the vehicle temperature and speed remain constant, the variation of free-stream gas temperature would be expected to have practically no effect on measurements at the forward portion of the vehicle. The effect on regions near 90 degrees from the stagnation point would be more pronounced. However, in order to obtain accurate results for this effect, extensive and very long computer runs would have to be performed in order to reduce statistical scatter in this region of very low flux. This is particularly true at lower Knudsen numbers.

E. EFFECTS OF OTHER PARAMETERS

Effects of other parameters, such as mass ratio and mixture ratio, are not as pronounced as those of Knudsen number. However, from the limited information so far obtained, certain general trends can be predicted.

- Increasing mass ratio generally increases species separation near the stagnation point.

- Increasing the mole fraction of the light species generally decreases the species separation effect (i.e., the heavy species are not as overabundant when the light species is a major constituent).

F. INTERNAL FLOW CONCLUSIONS

Preliminary information has been obtained on the conditions inside an instrument cavity consisting of a long tube with a constriction at the entrance (see Figure 24a) and with the incoming flux distribution corresponding to the external flow results. Two effects are noteworthy.

1. There appears to be a consistent flux rise with increased distance from the entrance, suggesting that the model of thermal equilibrium within the cavity is not very good for this geometry.

2. The transmission coefficients in the forward and reverse directions across the entrance regions are very nearly equal. If the usual model of a highly peaked, free-stream, incoming distribution function and an outgoing distribution function in thermal equilibrium with the cavity walls were used, the forward-to-reverse transmission coefficient ratio would be near 2. This results in a lower prediction of the cavity-pressure rise over the free-stream value than that obtained on the basis of free-molecular theory.

SECTION VI

RECOMMENDATIONS FOR FUTURE WORK

Now that a functional three-dimensional external flow computer program exists and is coupled with a functional three-dimensional internal flow computer program, future work in two fields is recommended. Improvements in the model used in the computer program should be continued. However, the present programs can also be used as they currently exist in order to give immediate engineering help in the design of experiments for satellites which will operate in the transitional flow regime. Details of these recommendations follow.

A. IMPROVED COMPUTER-PROGRAM MODEL

While the current programs give adequate results for all of the atmospheric conditions and geometries tested, certain simplifying approximations and limitations were incorporated. More accurate reduction of data, for satellites and rockets in the 90 to 150 kilometer altitude range, will result from an investigation of these limitations, and their effects should be considered. Three important effects, which were not included in the existing program, should receive emphasis:

1. The approximation of a binary gas mixture, while suitable for many analyses, should be refined to include such physical processes as dissociation and chemical reaction. Analysis of the local alteration of the gas composition by these processes will require provision for three significant species (i.e., two reacting species plus an inert background gas).
2. Collisional cross-sections are velocity dependent rather than constant, as assumed in the current program.
3. Molecules contain internal structure (such as rotational and vibrational states). Therefore, translational energy is not necessarily conserved in all collisions. The current program assumes hard sphere molecules with only energy of motion being conserved.

An improved program which includes the above considerations, will result in more confidence in the data analysis, and could improve the accuracy of the reduced data by as much as 25 percent.

B. CURRENT ENGINEERING DESIGN

Both of the current three-dimensional programs are developed to the point where they can be of practical use in the design and placement of experiments on satellites and rockets operating in the transitional flow regime of the atmosphere. Specifically, they can be applied to the design and integration of certain experiments scheduled to fly on Atmosphere Explorers C, D, and E.

All of the following information is obtainable from the existing programs:

1. Determination of the effect of perigee altitude on measurement errors arising from the fluid environment of the satellite.
2. Optimization of position of the instrument on the satellite.
3. The effect on measured data of varying the size and shape of any instrument cavity and its orifice.

Most of the above information will be obtained by using the internal flow program. The external flow program will be used primarily to compute the initial velocity samples at various altitudes.

SECTION VII

REFERENCES

1. Bird, G.A., "Shock Wave Structure in a Rigid Sphere Gas," Rarefied Gas Dynamics (ed J.H. deLeuw), Academic Press, Vol. I, p. 216. New York, 1965.

2. "Study of Flow Fields in the Transitional Regime and Their Effects Upon Aeronomy Measurements," GSFC Report No. CR-94922, issued by RCA Corp., May 17, 1968.

3. Bird, G.A., "Aerodynamic Properties of Some Simple Bodies in the Hypersonic Transition Region," AIAA Journal, Vol. 4, p. 55, (1966).

4. "Continuation of Low-Altitude Satellite Interaction Problem Investigation," GSFC Report No. CR-103666, issued by RCA Corp., June 18, 1969.

5. "GSFC Specification for Atmosphere Explorers AE-C and D" GSFC Specification No. S620-P-1, April, 1969.

6. "Program Report: EXT, A Program Which Models Supersonic Binary Gas Flow at any Angle of Attack Past a Body Composed of Rotated Conic Sections, Which is Comparable in Size to the Mean Free Path. INT, A Program Which Models Supersonic Binary Gas Flow at any Angle of Attack into a Cavity Composed of Rotated Conic Sections," issued by RCA Corp. for NASA/GSFC on Contract No. NAS 5-11241 on August 31, 1970.

7. "Low-Altitude Satellite Interaction Problem Investigation, Program Report," issued by RCA Corp. for NASA/GSFC on Contract No. NAS 5-11145 on November 1, 1968.

8. Data for the various altitudes were obtained from the Spring/Fall Model Tables of the "U.S. Standard Atmosphere Supplements, 1966," U.S. Government Printing Office, Washington, D.C. (1966).

9. Hughes, P.C., and de Leuw, J. H., "Theory for the Free Molecule Impact Probe at an Angle of Attack", Rarefied Gas Dynamics, Academic Press, Supplement 3, Vol. I, p. 653, New York, 1965.